Quaternary International 551 (2020) 7–28

Contents lists available at ScienceDirect

Quaternary International

journal homepage: www.elsevier.com/locate/quaint

An overview of Alpine and Mediterranean palaeogeography, terrestrial ecosystems and climate history during MIS 3 with focus on the Middle to Upper Palaeolithic transition

Federica Badino[a,b,*], Roberta Pini[b], Cesare Ravazzi[b], Davide Margaritora[b], Simona Arrighi[a,c,d], Eugenio Bortolini[a], Carla Figus[a], Biagio Giaccio[b,e], Federico Lugli[a,f], Giulia Marciani[a,d], Giovanni Monegato[g], Adriana Moroni[c], Fabio Negrino[h], Gregorio Oxilia[a], Marco Peresani[i], Matteo Romandini[a,i], Annamaria Ronchitelli[c], Enza E. Spinapolice[j], Andrea Zerboni[k], Stefano Benazzi[a,l]

[a] Dipartimento di Beni Culturali, Università di Bologna, 48121, Ravenna, Italy
[b] C.N.R, Istituto di Geologia Ambientale e Geoingegneria, 20126, Milano, Italy
[c] Dipartimento di Scienze Fisiche Della Terra e Dell'Ambiente, Università di Siena, 53100, Siena, Italy
[d] Centro Studi sul Quaternario, 52037, Sansepolcro, Italy
[e] C.N.R., Istituto di Geologia Ambientale e Geoingegneria, 00015, Rome, Italy
[f] Dipartimento di Scienze Chimiche e Geologiche, Università di Modena e Reggio Emilia, 41125, Modena, Italy
[g] C.N.R, Istituto di Geoscienze e Georisorse, 35131, Padova, Italy
[h] Dipartimento Antichità, Filosofia e Storia, Università di Genova, 16126, Genova, Italy
[i] Dipartimento di Studi Umanistici, Sezione di Scienze Preistoriche e Antropologiche, Università di Ferrara, 44100, Ferrara, Italy
[j] Dipartimento di Scienze Dell'Antichità, Università Sapienza, 00185, Roma, Italy
[k] Dipartimento di Scienze Della Terra "A. Desio", Università Degli Studi di Milano, 20133, Milano, Italy
[l] Department of Human Evolution Max Planck Institute for Evolutionary Anthropology, 04103, Leipzig, Germany

ARTICLE INFO

Keywords:
Middle Upper Palaeolithic
Palaeoecology
Palaeoclimate
Marine Isotope Stage 3
Terrestrial records

ABSTRACT

This paper summarizes the current state of knowledge about the millennial scale climate variability characterizing Marine Isotope Stage 3 (MIS 3) in S-Europe and the Mediterranean area and its effects on terrestrial ecosystems. The sequence of Dansgaard-Oeschger events, as recorded by Greenland ice cores and recognizable in isotope profiles from speleothems and high-resolution palaeoecological records, led to dramatic variations in glacier extent and sea level configuration with major impacts on the physiography and vegetation patterns, both latitudinally and altitudinally. The recurrent succession of (open) woodlands, including temperate taxa, and grasslands with xerophytic elements, have been tentatively correlated to GIs in Greenland ice cores. Concerning colder phases, the Greenland Stadials (GSs) related to Heinrich events (HEs) appear to have a more pronounced effect than other GSs on woodland withdrawal and xerophytes expansion. Notably, GS 9-HE4 phase corresponds to the most severe reduction of tree cover in a number of Mediterranean records. On a long-term scale, a reduction/opening of forests throughout MIS 3 started from Greenland Interstadials (GIs) 14/13 (ca. 55–48 ka), which show a maximum in woodland density. At that time, natural environments were favourable for Anatomically Modern Humans (AMHs) to migrate from Africa into Europe as documented by industries associated with modern hominin remains in the Levant. Afterwards, a variety of early Upper Palaeolithic cultures emerged (e.g., Uluzzian and Proto-Aurignacian). In this chronostratigraphic framework, attention is paid to the Campanian Ignimbrite tephra marker, as a pivotal tool for deciphering and correlating several temporal-spatial issues crucial for understanding the interaction between AMHs and Neandertals at the time of the Middle to Upper Palaeolithic transition.

* Corresponding author. Università di Bologna, Dipartimento di Beni Culturali, Via degli Ariani 1, 48121, Ravenna, Italy.
E-mail address: federica.badino@unibo.it (F. Badino).
URL: http://www.erc-success.eu/ (F. Badino).

https://doi.org/10.1016/j.quaint.2019.09.024
Received 31 January 2019; Received in revised form 16 July 2019; Accepted 17 September 2019
Available online 19 September 2019
1040-6182/

1. Introduction

Climate variability and landscape transformations underlie the complex interaction between natural resources and human dynamics. The understanding of these changes over time relies on palaeoclimate and palaeoecological information obtained from different natural archives (e.g. terrestrial and marine sediments, speleothems, ice cores, etc.), which are well known for their potential to record even abrupt and high frequencies events. The Marine Isotope Stage 3 (MIS 3, ca., 30-60 ka) in the last glacial period (Lisiecki and Raymo, 2005) is one of the most highly unstable phases, as far as climate is concerned, closely interwoven with the recent human evolution history. MIS 3 was characterized by major rapid climatic changes showing high variability, associated with abrupt atmospheric shifts over Greenland (Dansgaard-Oeschger [D-O] events) and episodes of massive iceberg discharge into the North Atlantic (Heinrich events [HEs]), enhancing cold and dry conditions at mid-to-low latitudes (Fletcher and Sánchez Goñi, 2008; Fleitmann et al., 2009; Naughton et al., 2009; Fletcher et al., 2010a).

Within this context, the Middle to Upper Palaeolithic transition (ca. 50–30 ka in Europe and western Asia, Higham et al., 2014; Benazzi et al., 2015; Hublin, 2015; Douka and Higham, 2017; Been et al., 2017; Margherita et al., 2017) represents one of the pivotal phases in human evolution documenting the demise of the autochthonous Neandertals and their replacement by Anatomically Modern Humans (AMHs). Many authors

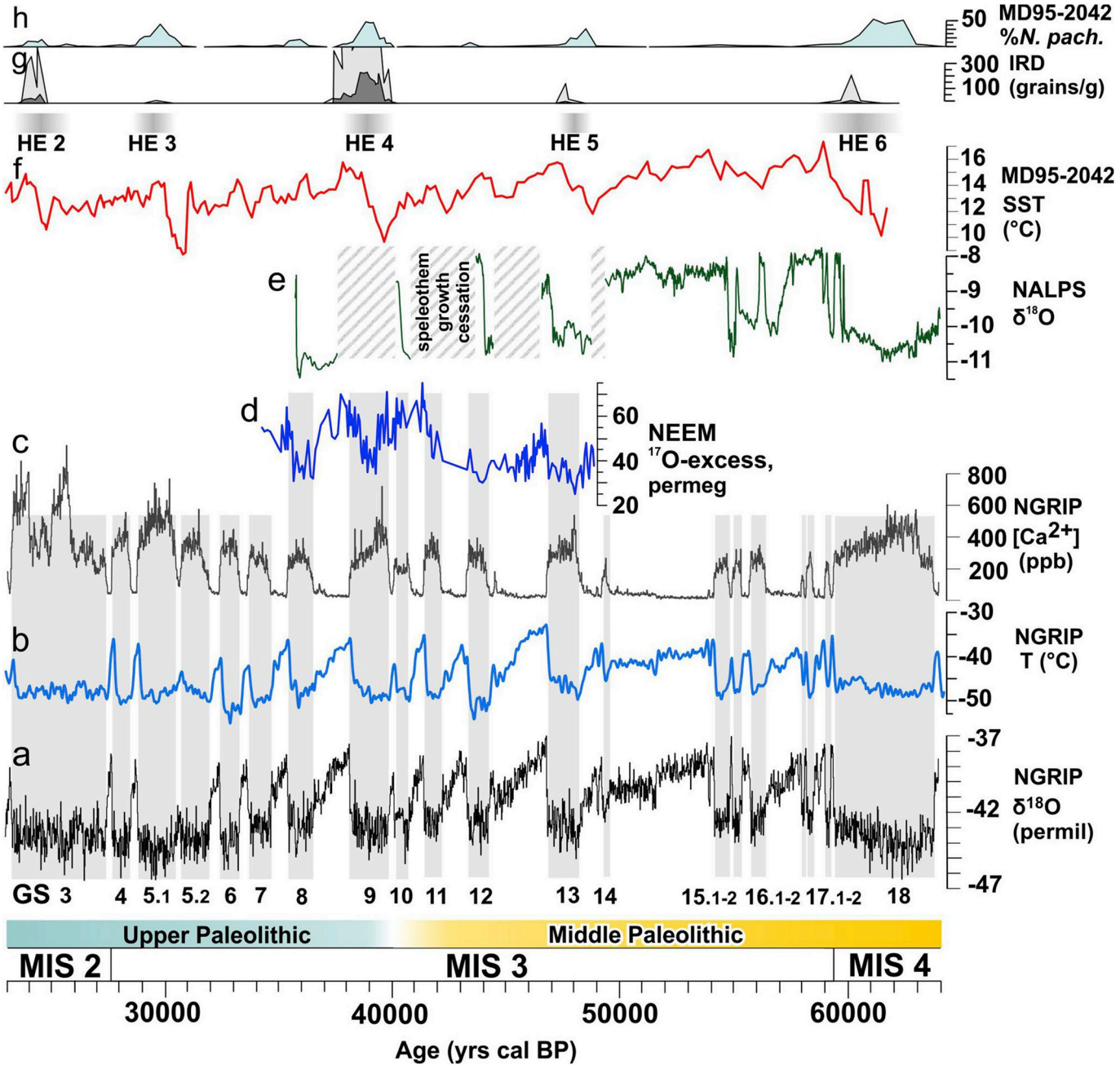

Fig. 1. Comparison of Northern Hemisphere terrestrial and marine paleoclimate proxies: (a) NGRIP $\delta^{18}O$ record (Rasmussen et al., 2014), (b) temperature reconstruction based on $\delta^{15}N$ (Kindler et al., 2014) and (c) calcium ion concentration ($[Ca^{2+}]$) record (Rasmussen et al., 2014), plotted all on the GICC05modelext chronology (Rasmussen et al., 2014); (d) NEEM ^{17}O-excess permeg (Guillevic et al., 2014); (e) $\delta^{18}O$ record from Northern Alps (NALPS) speleothems (Moseley et al., 2014) plotted on its timescale; (f) MD95-2042 Sea Surface Temperature record (Darfeuil et al., 2016), (g) *Neogloboquadrina pachyderma* abundance and (h) Ice-Radfted Debris record (Sánchez Goñi et al., 2008), plotted each on their own timescale. Vertical grey bars indicate Greenland Stadial (GS). Heinrich events (HEs) are indicated according to MD95-2042 chronology (Sánchez Goñi et al., 2008).

suggest that the eastern Mediterranean region and, in turn, the Italian Peninsula, served as gateways for the immigration and spread of AMHs from Africa to western Eurasia (van Andel et al., 2003; Müller et al., 2011; Moroni et al., 2013, 2018), where various transitional technocomplexes (eg., the Uluzzian in Italy and Greece, the Châtelperronian in central and south western France and northern Spain, the Neronian in south eastern France) replaced pre-existing Mousterian cultures (Mellars, 2006). Neandertals and AMHs societies developed in a context of continuous climatic fluctuations between cold-arid (Greenland Stadial, GS) and mild-humid (Greenland Interstadial, GI) conditions (Staubwasser et al., 2018). Surprisingly, despite the apparent body adaptations to live under rigid climates conditions (Steegmann et al., 2002), e.g., a wide and tall nasal aperture useful in humidifying and warming cold and dry air (Franciscus, 1999; Wroe et al., 2018), Neandertals did not survive into the coldest phases of MIS 3. Their extinction is statistically placed around 40 ka cal BP (Higham et al., 2014) and almost in coincidence with Greenland Stadial 9/HE 4, which is a noticeable cold phase recorded in both marine and terrestrial records (e.g. Fedele et al., 2003; Guillevic et al., 2014 and references therein). Several hypotheses have been proposed about Neandertal extinction and AMHs replacement, and the debate is still unresolved (e.g., Mellars, 2006; Hoffecker, 2009; Benazzi et al., 2011, 2015; Villa and Roebroeks, 2014; Higham et al., 2014; Hublin, 2015; Rey-Rodríguez et al., 2016; Greenbaum et al., 2019).

To disentangle the role played by climate, ecosystem changes and physiography in such human processes, a palaeoclimate and palaeoecological perspective focusing on Europe and the Mediterranean area is essential. These efforts represent part of a wider interest in determining how climate changes modified past environments.

The aim of this paper is to present the state-of-the-art of palaeoclimate and palaeoecological researches relevant to the ERC Consolidator Grant 2016 "SUCCESS - *The earliest migration of Homo sapiens in southern Europe: understanding the biocultural processes that define our uniqueness*". To contribute to the discussion about the arrival of AMHs in Southern Europe, the pattern of their diffusion and their interactions with Neandertals, a review of the current knowledge about the climate context and the landscape structure is presented. A selection of high-resolution palaeoecological records covering the time span between HE 5 to 3, known for their strong impact in western Eurasia, are discussed to explore the effects of short-term climate variability on ecosystems and human interactions.

2. Reference climate records for the last glacial period and signal synchronicity between different realms

2.1. MIS 3 as recorded in Greenland ice cores

MIS 3, which lasted from 60 ka to 30 ka, was characterized by millennial-scale climate oscillations commonly referred to as Dansgaard-Oeschger (D-O) events. These events, particularly well-defined in Greenland ice cores, were first described by Dansgaard et al. (1993). Typically, D-O events are featured by an abrupt transition (within a few decades) from a cold phase (GS), into a warm phase (GI). NGRIP, GRIP and GISP2 ice cores provide master records for these rapid climatic changes throughout the Last Glacial cycle (MIS 5d to the end of MIS 2; ca. 116–11.7 ka) in the North Atlantic region (McManus et al., 1999). Boundaries between GS and GI phases were established based on both stable-oxygen isotope ratios of the ice ($\delta^{18}O$, reflecting mainly local temperature) and calcium ion concentrations ($[Ca^{2+}]$ reflecting mainly atmospheric dust loading) measured in the ice (Fig. 1, a-c) (Rasmussen et al., 2014). The close timing of $\delta^{18}O$ and $[Ca^{2+}]$ abrupt shifts is also indicative of reorganisations in atmospheric circulation (Steffensen et al., 2008). Notably, $[Ca^{2+}]$ data reflect primarily changes in dust concentration but also changes in dust source conditions and transport paths (Fischer et al., 2007a, 2007b). During D-O events North Atlantic region temperature and East Asian storminess were tightly coupled and changed synchronously with no systematic lead or lag (Ruth et al., 2007), thus providing instantaneous climatic feedback. This relationship was stable over the entire Last Glacial period.

According to Petersen et al. (2013), the driving mechanism of GIs onset is linked to the rapid collapse of an ice-shelf fringing Greenland, potentially due to subsurface warming. During GI, a gradual cooling controlled by the timing of ice-shelf regrowth leads to GS conditions that lasted for centuries up to millennia. NGRIP temperature reconstructions based on $\delta^{15}N$ isotope measurements (Fig. 1, b) show T increase at the onset of each GI ranging from 6.5 °C (D-O 9) up to 16.5 °C (D-O 11), with an uncertainty of ± 3 °C (Kindler et al., 2014).

A recent important step forward is represented by the development of the ice-core GICC05 chronology (Andersen et al., 2006; Rasmussen et al., 2006; Svensson et al., 2008; Seierstad et al., 2014) and its flow model-based extension (GICC05modelext) published in Rasmussen et al. (2014), which allowed to achieve a reference template for the pattern of climate variability during the Last Glacial cycle.

2.2. Climate signals in mid-to low-latitude marine records

A well-known feature in North Atlantic marine sediments is the presence of coarse sediment layers, i.e. the ice-rafted debris (IRD, Ruddiman, 1977). Such depositional episodes, known as Heinrich Events (HE), are related to massive discharge, rafting and melting of icebergs into the ocean and the consequent fall of detrital sediments trapped in the ice on the ocean floor (Heinrich, 1988) and unambiguously identified during GS phases of the Last Glacial period (e.g. Bond et al., 1992, 1993; Hemming, 2004).

It is widely assumed that D-O events and HE are linked to reorganisations and/or variations in the strength of the Atlantic Meridional Overturning Circulation (AMOC) (Broecker et al., 1990). Specifically, Bagniewski et al. (2017) suggest a 30–50% weakening of the AMOC during GSs and a complete shutdown during HEs, also coinciding with large increases in the abundance of foraminifer polar species (e.g. *N. pachyderma*, Fig. 1h–g). The Iberian Margin (Fig. 1) is a key area for the reconstruction of these dynamics thanks to its distal position, i.e. outside of the main belt of ice rafting, which limit disturbance of the sediments (Bard et al., 2000; Pailler and Bard, 2002). The recently obtained Sea Surface Temperature (SST) curve based on the biomarker TEX_{86}^{H} in MD95-2042 core (Darfeuil et al., 2016) highlights that the greater cooling peaks occurred during HEs (about 3–5 °C; Fig. 1, f). This feature is in disagreement with the general pattern emerging over Greenland, where temperatures reconstructed during GS are roughly comparable and show more stable values to each other (Fig. 1, b). In addition, Martrat et al. (2007) argue that SST changes occur a few centuries before the subsequent generation of icebergs, which are traced by increases in IRD percentage. Regarding this issue, various studies state that HEs are shorter (Roche et al., 2004; Peters et al., 2008) than the corresponding GS and occur after the AMOC entered a weakening trend (Flückiger et al., 2006; Marcott et al., 2011). Thus, HEs seem to be a consequence rather than the cause of the AMOC weakening (e.g., Alvarez-Solas et al., 2010, 2013; Marcott et al., 2011; Barker et al., 2015).

Given the uncertainty across the North Atlantic in the ocean reservoir correction (e.g., Stern and Lisiecki, 2013; Butzin et al., 2017), and the lack of a clear HE signature in the $\delta^{18}O$ Greenland isotopic record (Rasmussen et al., 2014), it is difficult to establish where HEs lie exactly within the D-O framework (Andrews and Voelker, 2018). Indeed, Rasmussen et al. (2014) did not designate the temporal positions of HEs. However, new Greenland ice cores proxy records (e.g., ^{17}O-excess; Fig. 1, d) seem to be mostly linked to a lower-latitude hydrological cycle signal (Guillevic et al., 2014). This might help in the future to better constrain HEs in the ice core series, allowing to explore time leads and lags in between events happening at different latitudes.

2.3. Synchronicity between abrupt Greenland events and terrestrial responses in Southern Europe

Over the last two decades, the INTIMATE project (INTegrating Ice-core, MArine, and TErrestrial records; e.g., Blockley et al., 2012;

Rasmussen et al., 2014) has proposed a series of event-stratigraphic templates based on the isotopic and dust concentration changes in Greenland ice cores. The alternating pattern of stadial and interstadial geologic-climatic units, due to their very high stratigraphic and temporal resolution and precise dating, constitute the most comprehensive and best resolved archive of high-frequency climate variability. The Northern-Hemisphere transmission of such millennial-scale signals (reflected in $\delta^{18}O$ variations) depends on the extremely rapid atmospheric circulation changes (probable lag a couple of years only; Rasmussen et al., 2014). These changes are induced by migration of the Polar Front (PF) and shifts of the Intertropical Convergence Zone (ITCZ) at mid-to-low-latitudes (Europe and the Mediterranean areas) (e.g., Peterson and Haug, 2006), which in turn induce atmospheric circulation and local rainfall changes.

Problems in synchronization of MIS 3 records mainly arise from the uncertainties of the age modelsbased on different dating methods, the intrinsic difficulties in dating these events, in particular for those intervals at or beyond the limit of the radiocarbon technique (see section 7.1), and the scarcity of precisely dated and unambiguously synchronous stratigraphic events (e.g., tephra layers, magnetic excursions and cosmogenic nuclide peaks). Speleothems are excellent archives for recording these abrupt isotopic changes (e.g., Fleitmann et al., 2009; Moseley et al., 2014; Weber et al., 2018), since they are among the most accurately datable archives, i.e., within the last ca 100 ka, two sigma (95%) errors can be below 1% of the U/Th age. Their deposition is predominantly influenced by either temperature (higher latitude) or precipitation (lower latitude), but both ultimately linked to Northern Hemisphere temperature fluctuations (e.g., McDermott, 2004; Genty et al., 2006). In general, speleothem records unambiguously show the signature of D-O cycles and HEs on European and Mediterranean climate, and a millennial to sub-millennial scale synchronicity in climatic shifts between European and Greenland isotopic records. Despite a generally continuous calcite deposition during the GI 14-GI 13 interval, even at the elevation of the modern snowline in the Alps (Spötl and Mangini, 2007; Moseley et al., 2014), speleothems registration is often fragmentary and hiatuses may have occurred during cold/dry phases (i.e. HE 5 and HE 4; Spötl et al., 2002; Moseley et al. 2014, Fig. 1, e; Weber et al., 2018). In fact, ITCZ variations may have also affected local rainfall patterns, triggering enhanced dryness notably in the Mediterranean (Fletcher and Sánchez Goñi, 2008; Fleitmann et al., 2009). However, precise determination of the durations of these hiatuses may provide valuable information about climatic thresholds that affect regional climatic conditions (Moreno et al., 2010; Zhornyak et al., 2011; Stoll et al., 2013). Overall, the climatic pattern underlying these $\delta^{18}O$ profiles during MIS 3 strongly resembles that of Greenland ice cores at millennial scales, and in many cases corresponding to the detail of decadal-scale cooling events within interstadials (Moseley et al., 2014).

3. Reference mid-to-high resolution MIS 3 palaeoecological records in Southern Europe and in the Mediterranean region

Palaeoecological and palaeoclimate archives considered in this review paper (Table 1) are mostly located in Southern Europe and in the Mediterranean region between ca. 36° and 46.5° N throughout the Atlantic, Continental, Alpine, and Mediterranean biogeographical regions (Fig. 2; European Environment Agency, 2015). A few other datasets from central Europe accompany these sites. Selected records (i) cover a relevant interval during the ca. 30–60 ka time-frame, (ii) are mostly characterized by a sub-millennial/multi-decadal time resolution (see Table 1), and (iii) include quantitative or semi-quantitative geochemical (i.e., stable isotopes) and/or vegetation (i.e. palynological data) climate proxy variables. Most of them are placed in the Mediterranean region, which borders the Atlantic region in the west and the western Eurasian sub-continental region including both the Black Sea and the Anatolian regions (Fig. 2). The latter area is of particular interest because it possibly served as a gateway for the spread of AMHs into Europe (Müller et al., 2011). Thus, palaeoclimatic and palaeoecological information from these sites are of great importance and serve as background for the archaeological work in the Levant.

3.1. Vegetation response to D-O events and HEs in Southern Europe and Mediterranean region

The history of vegetation during MIS 3 in Southern Europe and in the Mediterranean area relies on several palaeoecological studies carried out in lake and peat stratigraphic sequences. In Fig. 3 we consider the evidence for millennial-scale variability and long-term vegetation trends from selected records covering the period between ca. 60 - 30 ka (i.e., GI 17 to GI 5). The records are presented on the most recent chronology available for each one. On the whole, this data shows a high sensitivity of vegetation response to D-O events, making South Eastern Europe and the Italian Peninsula a key geographical area for high-resolution palaeoenvironmental researches during the last glacial period.

In southern Europe, the recurrent succession of (open) woodlands, including temperate taxa, and grasslands with xerophytic elements (Fig. 3), have been tentatively correlated to GIs in Greenland ice cores (Fletcher et al., 2010b). This assumption is reasonable for this geographic area as thermophilous trees persisted in refugia and appeared to have expanded rapidly during each interstadial without substantial migration lags (Harrison and Sánchez Goñi, 2010).

Investigations at Lago Grande di Monticchio (Allen et al., 1999, 2000) were the first to provide an independently dated Late Pleistocene palaeoenvironmental record, due to its varved sequence. Furthermore, the identification of known tephra layers, one of which is the Campanian Ignimbrite (CI), has also been used to improve the age-depth model (Wutke et al., 2015). The high-resolution pollen record (ca. 200 yrs/sample) obtained from the Monticchio core reveals millennial-scale changes in woody/open environments throughout MIS 3. Palaeoecological data indicate an alternation between cold/dry steppic vegetation, referred to GS periods, and an increased range of woody taxa including deciduous *Quercus*, *Abies* and *Fagus* (up to 30–60% AP), referred to GIs (Allen et al., 1999; Fletcher et al., 2010b). Similarly, other long pollen records from volcanic lakes in central and southern Italy, i.e., Lagaccione and Valle di Castiglione (Fig. 3; Follieri et al., 1988, 1998; Magri, 1999), show remarkable changes in vegetation composition, structure and biomass including millennial-scale fluctuations in forest development with deciduous and evergreen *Quercus, Corylus, Fagus*, *Betula* and *Picea* (Fletcher et al., 2010b). The lower temporal resolution of these latter records (ca. 400 yr/sample) in turn reduced the chances to precisely identify each GI (Fig. 3).

In northern Italy, pollen records from Lake Fimon (Fig. 3) and Azzano Decimo (Pini et al., 2009, 2010) indicate phases of conifer-dominated forest expansion (*Pinus sylvestris-mugo* and *Picea*), rich in cool broad-leaved trees (*Alnus* cf. *incana* and tree *Betula*) and accompanied by a reduced warm-temperate component (*Tilia*). In both records, individual D–O events cannot be identified due to the low temporal resolution (ca. 800–1000 yr/sample), nevertheless the well-documented long vegetation trend is indicative of a persistent afforestation. In fact, only moderate forest withdrawals occurred and some temperate trees (e.g., *Tilia* and *Abies*) persisted up to ca. 40 ka BP (Pini et al., 2010). Interestingly, peaks of *Tilia* pollen were found (Cattani and Renault-Miskovsky, 1983–84) in layers preserving Mousterian artefacts and dated to 40.6–46.4 ^{14}C ka in the cave sediments at the Broion shelter (Leonardi and Broglio, 1966), and also in Paina cave inter-pleniglacial deposits (Bartolomei et al., 1987–88; Cattani, 1990).

At southern latitudes, high-resolution pollen records from Ioannina, Tenaghi Philippon and Megali Limni (Greece, Figs. 2 and 3; Wijmstra, 1969; Tzedakis et al., 2006; Margari et al., 2009; Müller et al., 2011; Wulf et al., 2018) show exceptional series of millennial and sub-millennial vegetation changes correlated to a number of GI/GS (Fletcher et al., 2010b; Pross et al., 2015). Concerning colder phases, the GSs related to HEs appear to have a more pronounced effect than other GSs on woodland withdrawal and xerophytes expansion. Notably, GS 9-HE

Table 1
List of selected sites from S-Europe and the Mediterranean area that entirely or partially cover the MIS 3 chronological framework, specifying location, available vegetation-climate proxy variables and time resolution. References to published data are also indicated.

Site	Archive type	Latitude (decimal degrees)	Longitude (decimal degrees)	Elevation (m asl)	Interval/Time period (ka)	Palaeoenvironmental /climate proxies	Mean temporal resolution for MIS 3 (yrs/sample)	References
TERRESTRIAL								
Abric Romani (Spain)	Carbonate sediments/ travertine deposits	41.53	1.68	310	41-70 ka	Palynological data	200 yrs	Burjachs et al. (2012)
Azzano Decimo (Italy)	Lake sediments	45.85	12.9	10	0-215 ka (discontinuous)	Palynological data	1150 yrs	Pini et al. (2009)
Lac du Bouchet (France)	Lake sediments	44.83	3.82	1200	ca. 8–120 ka	Palynological data	ca. 1000 yrs	Reille and Beaulieu (1990)
Eifel maar (Germany)	Lake sediments	50.16	6.85	420	0-60 ka	Palynological data	Decadal/centennial	Sirocko et al. (2016)
Fimon (Italy)	Lake sediments	45.46	11.53	23	27-138 ka	Palynological data	960 yrs	Pini et al. (2010)
Füramoos (Germany)	Peat deposits	47.98	9.88	662	0-14 ka, 40–140 ka	Palynological data	ca. 900–1200 yrs	Müller et al. (2003)
Ioannina 284 (Greece)	Lake sediments	39.75	20.85	470	0-132 ka	Palynological data	325 yrs	Tzedakis et al. (2002)
La Grand Pile (France)	Lake sediments	47.73	6.50	330	0-140 ka	Palynological data	ca. 250 yrs	Woillard (1978); Guiot et al. (1992)
Lagaccione (Italy)	Lake sediments	42.57	11.8	355	4-100 ka	Palynological data	420 yrs	Magri (1999)
Les Echets (France)	Lake sediments	45.9	4.93	267	ca. 10–75 ka	Palynological data	ca. 500 yrs	Beaulieu and Reille (1984)
Kopais K-93 (Greece)	Lake sediments	38.43	23.05	95	10-130 ka	Palynological data	830 yrs	Tzedakis (1999)
Megali Limni (Greece)	Lake sediments	39.1	26.32	323	22-62 ka	Palynological data	150 yrs	Margari et al. (2009)
Lago Grande di Monticchio (Italy)	Lake sediments	40.93	15.62	656	0-132 ka	Palynological data	210 yrs	Allen et al. (1999); Wutke et al. (2015)
Ohrid (Republic of Macedonia and Albania)	Lake sediments	40.91	20.67	693	0-500 ka	Palynological data	ca. 850 yrs	Sadori et al. (2016)
Prespa (Republic of Macedonia, Albania and Greece)	Lake sediments	40.95	20.96	849	0-92 ka	Palynological data	ca. 1070 yrs	Panagiotopoulos et al. (2014)
Ribains (France)	Lake sediments	44.83	3.82	1075	10-150 ka	Palynological data	ca. 1500 yrs	Beaulieu and Reille (1992b)
Tenaghi Phillippon (TF II) (Greece)	Peat-dominated succession	41.17	24.33	40	0-130 ka	Palynological data	120 yrs	Wijmstra (1969); Müller et al. (2011); Wulf et al. (2018)
Valle di Castiglione (Italy)	Lake sediments	41.88	12.77	44	0-250 ka	Palynological data	440 yrs	Follieri et al., 1988-1998
Lago di Vico (Italy)	Lake sediments	42.32	12.28	507	0-90 ka	Palynological data	ca. 500 yrs	Leroy et al. (1996); Magri and Sadori (1999).
Bunker cave - Bu2 (Germany)	Speleothems	51.36	7.6	184	From 52 to 50.9 ka and from 47.3 to 42.8 ka	Calcite $\delta^{18}O$, $\delta^{13}C$	decadal/multidecadal-scale	Weber et al. (2018)
Hölloch cave (Höl-7, Höl-16, Höl-17, and Höl-18) - NALSP (Germany)	Speleothems	47.38	10.15	1240–1438	35-65 ka (discontinuous)	Calcite $\delta^{18}O$, $\delta^{13}C$	decadal/multidecadal-scale	Moseley et al. (2014)
Kleegruben cave - SPA 49 (Austria)	Speleothems	47.09	11.67	2165	46-58 ka	Calcite $\delta^{18}O$, $\delta^{13}C$	decadal/multidecadal-scale	Spötl et al. (2002)
Soreq cave (Israel)	Speleothems	31.7	35	400	0-60 ka	Calcite $\delta^{18}O$, $\delta^{13}C$	40 yrs	Bar-Matthews et al., 1999-2000
Villars cave - Vil 27 (France)	Speleothems	45.3	0.5	175	30-55 ka	Calcite $\delta^{18}O$, $\delta^{13}C$)	53 yrs (between 48.5 and 40.5 ka) and 203 yrs (between 40.5 and 30 ka)	Genty et al. (2010)
Villars cave - Vil 9 (France)	Speleothems	45.3	0.5	175	32-83 ka (discontinuous)	Calcite $\delta^{18}O$, $\delta^{13}C$	91 yrs (between 51.8 and 40.4 ka) and 195 yrs (between 40.4 and 31.8 ka)	Genty et al. (2003)
Villars cave - Vil 14 (France)	Speleothems	45.3	0.5	175	29-52 ka	Calcite $\delta^{18}O$, $\delta^{13}C$	81 yrs (between 52.2 and 41.7 ka) and 1066 yrs (between 41.7 and 28.9 ka)	Wainer et al. (2009)
NGRIP (Greenland)	Ice core	75.1	42.32	2917	8-120 ka	$\delta^{18}O$; calcium ion concentration data([Ca2+])	re-sampled to 20-year resolution	Seierstad et al. (2014); Rasmussen et al. (2014)
MARINE								

(*continued on next page*)

Table 1 (*continued*)

Site	Archive type	Latitude (decimal degrees)	Longitude (decimal degrees)	Elevation (m asl)	Interval/Time period (ka)	Palaeoenvironmental /climate proxies	Mean temporal resolution for MIS 3 (yrs/sample)	References
MD04-2845 (Western France)	Marine sediments	45.35	−5.22	−4100	30-140 ka	Palynological data; Foraminiferal $\delta^{18}O$; Ice-rafted debris record	540 yrs	Sánchez Goñi et al. (2008)
MD95-2042 (Iberian margin)	Marine sediments	37.8	−10.17	−3148	27-138 ka	Palynological data; Foraminiferal $\delta^{18}O$; Ice-rafted debris record; UK'_{37} and TEX_{86} biomarkers (SST)	ca. 370 yrs	Sánchez Goñi et al., 1999-2000-2008-2009
MD95-2043 (Alboran sea)	Marine sediments	36.13	−2.62	−1841	0-50 ka	Palynological data; Foraminiferal $\delta^{18}O$; C_{37} Alchenones (SST)	260 yrs	Cacho et al. (1999); Sánchez Goñi et al. (1999); Fletcher and Sánchez Goñi (2008)
LC21 (Aegean sea)	Marine sediments	35.66	26.58	−1522	0-160 ka	Foraminiferal $\delta^{18}O$	ca. 200 yrs	Grant et al. (2012)
ODP 976 (Alboran sea)	Marine sediments	36.20	−4.30	−1108	> 1 Ma	Palynological data; Foraminiferal $\delta^{18}O$	Ranging between 50 and 200 yrs	Combourieu-Nebout et al. (2002); Combourieu-Nebout et al. (2009); Genty et al. (2010)

4 phase corresponds to the most severe reduction of tree cover in a number of records (e.g., Megali Limni, Tenaghi Philippon, Valle di Castiglione and Ioannina; Fig. 3). Interestingly, pollen records from different bioclimatic areas seem to show differences in terms of magnitude of response to cold events due to local ecosystem structures. In sites where moisture availability was not a limiting factor, differences in the magnitude of climate forcing during HEs seem to be well expressed in terms of major vegetation changes (e.g., Ioannina, Monticchio) (Fig. 3). However, where temperate tree populations were near their tolerance limit, the environmental stress associated with HEs probably crossed a critical threshold resulting in large population contraction with an almost complete reduction in forest cover (i.e., Tenaghi Philippon, Megali Limni) (Tzedakis et al., 2004) (Fig. 3).

On a long-term scale, a reduction/opening of forests throughout MIS 3 (see Fig. 3) took place from GI 14, showing a maximum in woodland density, and through the following GI 12 and GI 8. During GI 14/13 interval, conditions were notably humid and mild in the eastern Mediterranean as indicated by the Soreq cave isotopic record (Bar-Matthews et al., 2000) and also over Europe (Allen et al., 1999; Sánchez Goñi et al., 2002; Fletcher et al., 2010b).

Despite the relatively high amount of palaeoecological information for southern Europe, the spatial distribution of records in this heterogeneous geographic sector remains uneven. Such differences in the expression of millennial-scale events suggest that site characteristics need to be taken into account when mapping the spatial patterns of changes and trying to elucidate the mechanisms involved. New records are needed (e.g., from northern and southern Italy, Turkey, the Levant), in order to refine the knowledge of eco-climatic gradients across the continent and to better understand regional vegetation patterns.

3.2. Fire dynamics in Southern Europe and Mediterranean region

High-resolution microcharcoal records can provide new insights to understand fire-vegetation dynamics in relation to climate variability (e.g. D-O cyclicity/HE events) and/or human activities (e.g., Whitlock and Larsen, 2001; Iglesias et al., 2015). As for the Last Glacial period, few microcharcoal records are available from terrestrial (e.g., Magri, 2008; Margari et al., 2009; Pini et al., 2009, 2010) and marine records (e.g., Daniau et al., 2007, 2009). Fig. 3 shows microcharcoal data for some Southern East European terrestrial sites: Lake Fimon, Valle di Castiglione, Lagaccione and Megali Limni (MIS 3 partially documented).

Overall, a fire regime variability mainly associated with fluctuations in forest cover occurred between GS (lower fire activity) and GI (higher fire activity). Higher microcharcoal concentration during periods of afforestation suggests enhanced fire activity favoured by increasing woody fuel and biomass accumulation during GIs (Magri, 1994), as observed also by Daniau et al. (2007, 2009) for southwestern Iberia (MD95-2042 and MD04-2845 cores, Fig. 2). Contrary to this pattern, NE-Italy experienced isolated major fire episodes over a generally low-intensity fire regime; at Lake Fimon (Pini et al., 2010, Fig. 2) the strongest fire episode of the whole Late Pleistocene record is coeval to a drop in forest cover mirrored by steppe expansion, possibly correlated to HE4 (Fig. 3). Since the palaeoecological data from this site suggest relatively high moisture availability during MIS 3 (Pini et al., 2010), such climatic context may have prevented long-term fire activity south of the Alps, despite biomass availability. This evidence indicates that the incidence of fires is not always directly correlated with the degree of afforestation. This framework supports a regional climatic influence on fire regimes over SE-Europe with a direct climatic control on fuel availability during the last glacial period.

4. Snapshots of European palaeogeography and ecoclimatic zones during Greenland Interstadial 12 and the LGM

With the aim of setting Palaeolithic humans in a palaeoenvironmental scenario, we chose two MIS 3–2 key intervals relevant for the human

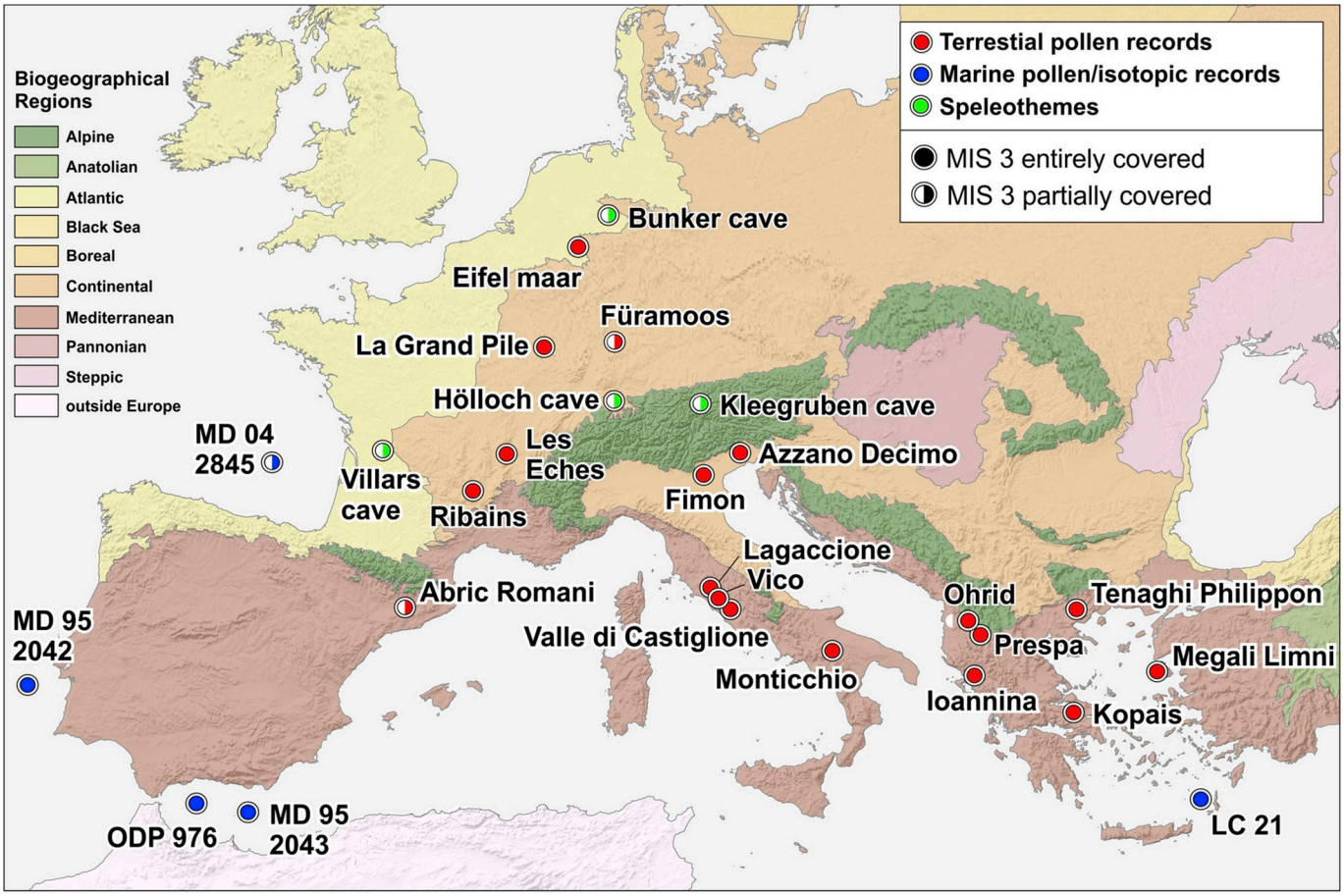

Fig. 2. European biogeographical map. Overview of mid-to high-resolution marine and terrestrial records entirely or partially covering MIS 3.

evolution and marking paleoclimate extreme conditions: the GI 12 and LGM. We plotted the main European palaeogeography and palaeoecology landscape features on geographical snapshots (Fig. 4A and B). In detail, GI 12 snapshot (ca. 46.8 to 44.2 ka according to Rasmussen et al., 2014) represents a phase of major forest expansion during MIS 3 also coincident with the AMHs arrival in Europe (Grotta del Cavallo, ca. 45.5 ka; Benazzi et al., 2011; Zanchetta et al., 2018) (Fig. 4A). The second one spans the time interval of both the SIS (Scandinavian Ice Sheet) and the European mountain glacier culminations during the LGM (26–21 ka cal BP in Europe, see Hughes et al., 2016; Monegato et al., 2017), which was characterized by one of the most pronounced forest contractions of MIS 3–2 time span (Fig. 4B). From GI 12 to LGM, climate changes led to dramatic variations in glacier extent and sea level with major impacts on the physiography of mountain areas, coastal regions and hydrologic systems. The latter two are also known for their important role in AMHs dispersal into Europe (Mellars, 2006; Hublin, 2014).

4.1. Palaeoenvironmental setting during GI 12

4.1.1. Reconstructed gradients ecogeography within eco-climatic zones

We reconstructed terrestrial ecosystems for a time frame corresponding to GI 12 (Fig. 4A) by combining palaeobotanical records (for Central Europe: see Van Meerbeeck et al., 2011 and references therein; Follieri et al., 1988; Beaulieu and Reille, 1992a-b; Drescher-Schneider et al., 2007; for Mediterranean Europe: Magri, 1999; Sánchez Goñi et al., 2002, 2009; Pini et al., 2009, 2010; Müller et al., 2011) and ecoclimatic gradients. These gradients rely both on large scale latitudinal zones (i.e., Tundra zone and Forest-tundra zone, and related positions of polar timberline, see Holtmeier, 1985; Archibold, 2012), spanning the northern half of European subcontinent and on regional elevational mountain belts in southern Europe (see Fig. 4A). We assumed GI 14 and GI 12 vegetation peaks to have been similar at the same site, although GI 12 was shorter, and used both GI 14 and GI 12 data to implement our reference dataset. Fossil data was improved by (a) elevational ecoclimatic relationships and (b) vegetation models (Alfano et al., 2003). However, available gridded vegetation models do not account for vegetation distribution in complex mountain regions that actually represent 75% (total areas above 500 m altitude obtained from GIS elaboration) of the southern European landscape. Indeed, elevation gradients can be very steep and, within a 1-km^2 grid cell, elevation can vary up to, or even more than, 500 m. In these contexts, forests display a characteristic discontinuity in their distribution with a main boundary representing the upper limit of forest canopies associated with temperature decrease along elevational gradients. Thus, some inaccuracies in the vegetation distribution can be expected in global models due to the coarse spatial resolution of climate datasets that can be affected by errors in the local temperature estimation (i.e., more than 1 °C for a lapse rate of about −0.5 °C/100 m).

A number of ecoclimatic zones are featured by distinct regional climates (i.e. coniferous and broad-leaved woodlands along the northern coast of Portugal and Spain; map of the European Environment Agency, 2015). Within each zone, local climates (i.e. mountain areas) have been qualified by elevational gradients of orographic precipitation. The main features of these altitudinal gradients are the upper timberline limit and the glacier Equilibrium Line Altitude. Given the determinants of the warmest month temperature (TJuly) on the upper timberline, caused by heat deficiency (Tranquillini, 1979; Jobbagy and Jackson, 2000; Körner and Paulsen, 2004), we used TJuly reconstructions for GI 12 to estimate the altitude of montane timberline. In order to moderate the effects of CO_2 changes on plant fertilization (Farquhar, 1997), we included past timberlines as calibration

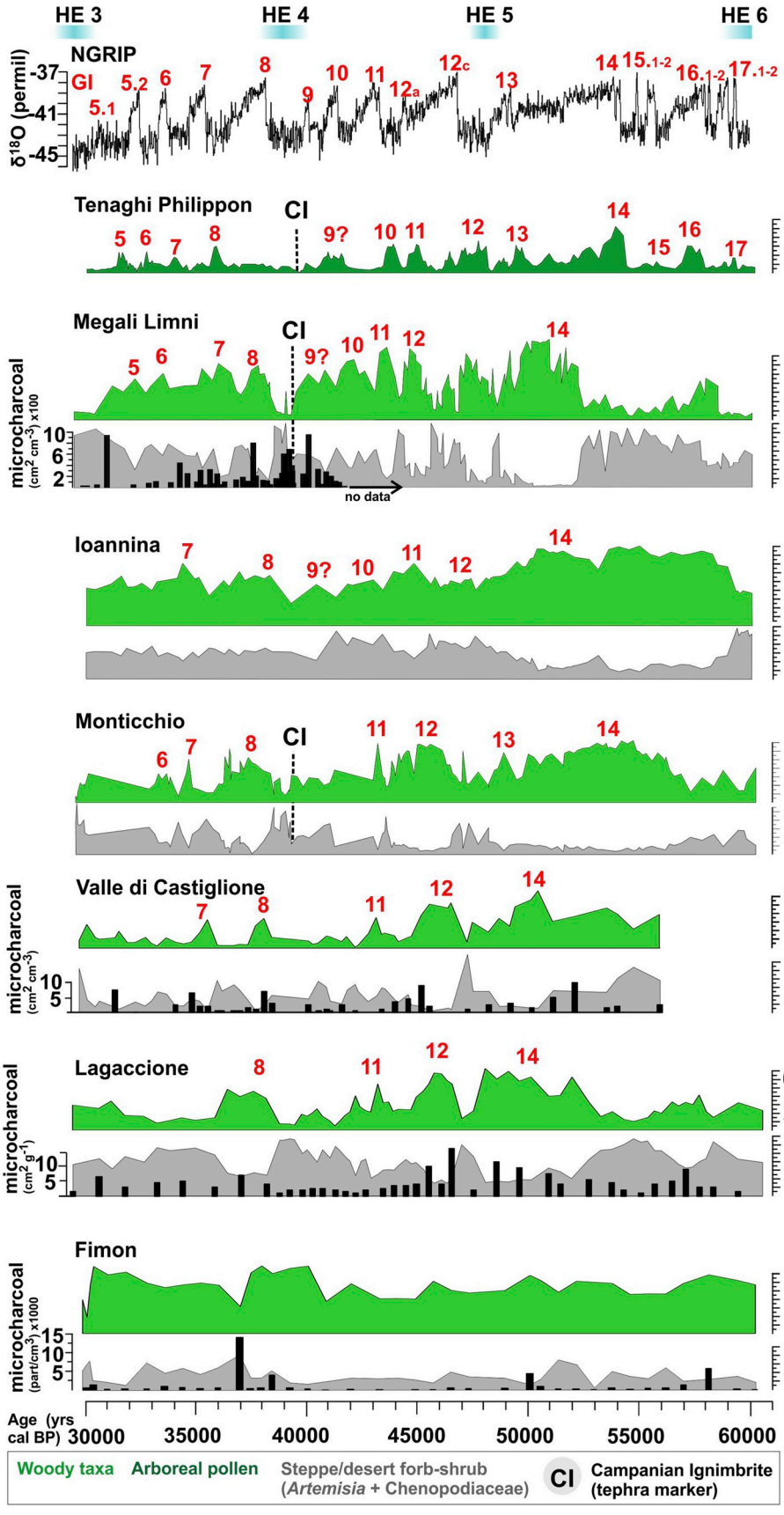

Biogeographical regions, physical and climate setting

Mediterranean region
(Greece)
Lat.: 41.17˚, Long.: 24.33˚
Altitude: 40 m asl
Present-day climate: Mediterranean; mean T January: 3.4 °C and mean T July: 23.9 ºC; mean annual P: 600 mm

Mediterranean region
(Greece, Lesvos island)
Lat.: 39.1˚, Long.: 26.32˚
Altitude: 323 m asl
Present-day climate: Mediterranean with mean T winter: 10.4 ºC; T summer: 26.1 °C; mean annual P: 725 mm - 415 mm (East to West)

Mediterranean region
(Greece)
Lat.: 39.75˚, Long.: 20.85˚
Altitude: 470 m asl
Present-day climate: sub-Mediterranean with high annual P and moderate summer drought; mean annual P: 1200 mm

Mediterranean region
(Italian peninsula)
Lat.: 40.93˚, Long.: 15.62˚
Altitude: 656 m asl
Present-day climate: wet winters with a pronunced dry period in summer; mean annual T: 13.7 ºC; mean annual P: 815 mm

Mediterranean region
(Italian peninsula)
Lat.: 41.88˚, Long.: 12.77˚
Altitude: 44 m asl
Present-day climate: mean annual T: 15ºC; mean annual P: 800 mm

Mediterranean region
(Italian peninsula)
Lat.: 42.57˚, Long.: 11.8˚
Elevation: 355 m asl
Present-day climate: mean annual T: 13.1 °C; maen annual P: 1030 mm

Continental region
(north-eastern Italy)
Lat.: 45.46˚, Long.: 11.53˚
Elevation: 23 m asl
Present-day climate: temperate-humid laking a dry season; mean annual T: 12.8 °C; mean annual P: 1038 mm

(caption on next page)

Fig. 3. Vegetation changes throughout MIS 3 in several high-to mid-resolution terrestrial pollen records from S-Europe and Mediterranean region. Pollen curves: % of woody taxa (sum of trees and shrubs) (light green); % of arboreal pollen (dark green); % of xerophytic elements (sum of *Artemisia* and Chenopodiaceae) (grey). Black histograms show pollen-slide microcharcoal concentrations. All records are plotted using the latest available chronology for each individual site. NGRIP $\delta^{18}O$ record is also shown (NGRIP members, 2004; Rasmussen et al., 2014). Red numbers indicate Greenland Interstadials (GI), modified from Fletcher et al., 2010a). Heinrich events (HEs) are indicated according to MD95-2042 chronology (Sánchez Goñi et al., 2008). (For interpretation of the references to colour in this figure legend, the reader is referred to the Web version of this article.)

test of our estimations. The timberline position in the Italian Central Alps during the Bølling-Allerød (1700–1800 m asl: Tinner et al., 1999; Ravazzi et al., 2007) is a good test as the GI 1 is the only D-O interstadial which occurred under moderately low CO_2 concentration; furthermore, relevant fossil records are relatively common as they were not erased by LGM glacier activity. Given the position of the alpine timberline during the Bølling-Allerød and the associated pollen-based mean TJuly (18,5–19 °C; Vallè et al., unpublished data), we infer the timberline position during GI 12 using the difference between TJuly for GI 12 (ca. 18 °C) and the Bølling-Allerød. This difference was projected over an elevational gradient using an average environmental lapse rate of about −0,67 °C/100 m (Furlanetto et al., 2019), to obtain an historical timberline for GI 12 (ca. 1600 m in the Italian Central Alps). The method was also tentatively applied to estimate timberlines in the Mediterranean region. Here, however, many boreal tree species were missing during MIS 3, thus ecophysiological requirements of Mediterranean timberline species were considered.

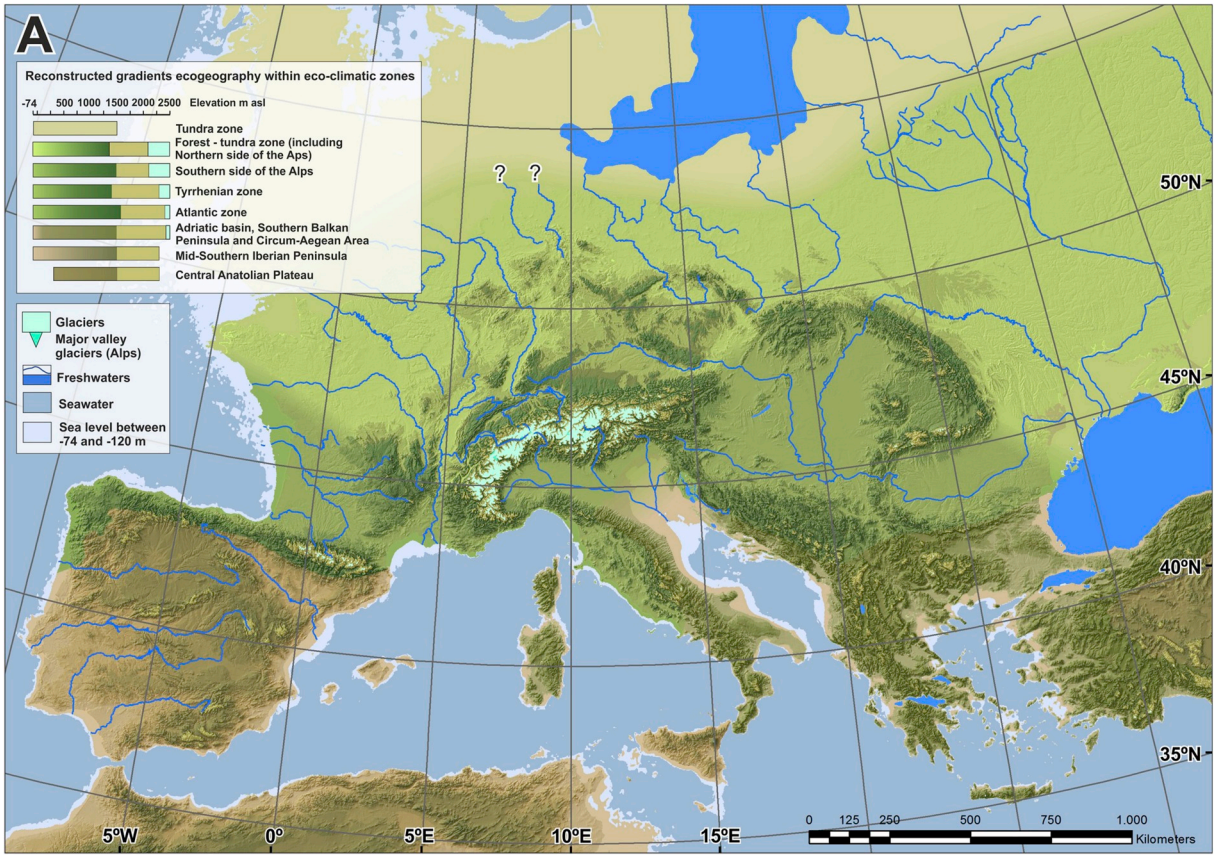

Fig. 4. A) Ecogeography of Greenland Interstadial 12 (GI 12; ca. 46.8 to 44.2 ka according to Rasmussen et al., 2014), showing reconstructed gradients within European eco-climatic zones. Digital Elevation Model (base topography – ETOPO, 2011; ETRS_1989_LAEA_152 projected coordinate system). Sea surface lowered to −74 m asl (Waelbroeck et al., 2002; Antonioli, 2012). Baltic lake drawn after Lambeck et al. (2010). The mountain glaciers (pale blue) and the main Alpine valley glaciers (cyan triangles) are inferred both from simulations (Seguinot et al., 2018) and ELA calculations, for more information see section 4.1.2. Colour scale bars depict eco-climatic zones gradients. Sharp limits mark reconstructed elevational timberlines position and mountain glaciers extent in different mountain systems within each eco-climatic zone, see sections 4.1 and 4.2. **B)** Palaeogeographic map of Europe during the Last Glacial Maximum. Digital Elevation Model (base topography – ETOPO, 2011; ETRS_1989_LAEA_152 projected coordinate system). Sea level drop at – 120 m (Pellegrini et al., 2017; 2018). Scandinavian and British Islands ice sheets (pale blue) after Hughes et al. (2016) at 22 ka. The mountain glaciers (pale blue) from Ehlers et al. (2011) with updated reconstructions in the Tatra Mountains (Zasadni and Klapyta, 2014), Dinarides (Kuhlemann et al., 2009; Žebre and Stepišnik, 2014, 2015; Temovski et al., 2018), Pyrenees (Delmas, 2015), Cantabrian range (Serrano et al., 2015). Alpine glaciers downloaded from https://booksite.elsevier.com/9780444534477/and modified in the Italian side using updated reconstructions (Ravazzi et al., 2012; Monegato et al., 2017; Gianotti et al., 2015; Ivy-Ochs et al., 2018; Rossato et al., 2018). Major European and eastern European lakes and rivers after Toucanne et al. (2015) and Verheul et al. (2015), Adriatic lakes (Miko et al., 2017) and rivers simplified from Maselli et al. (2014). Italian rivers draining major ice lobes at the outlet of alpine valleys are indicated with solid blue lines, outlined lines are used for lower-order rivers. Aeolian sediments (yellow polygons) based on data from compilations by Haase et al. (2007); Italian loess from Zerboni et al. (2018). (For interpretation of the references to colour in this figure legend, the reader is referred to the Web version of this article.)

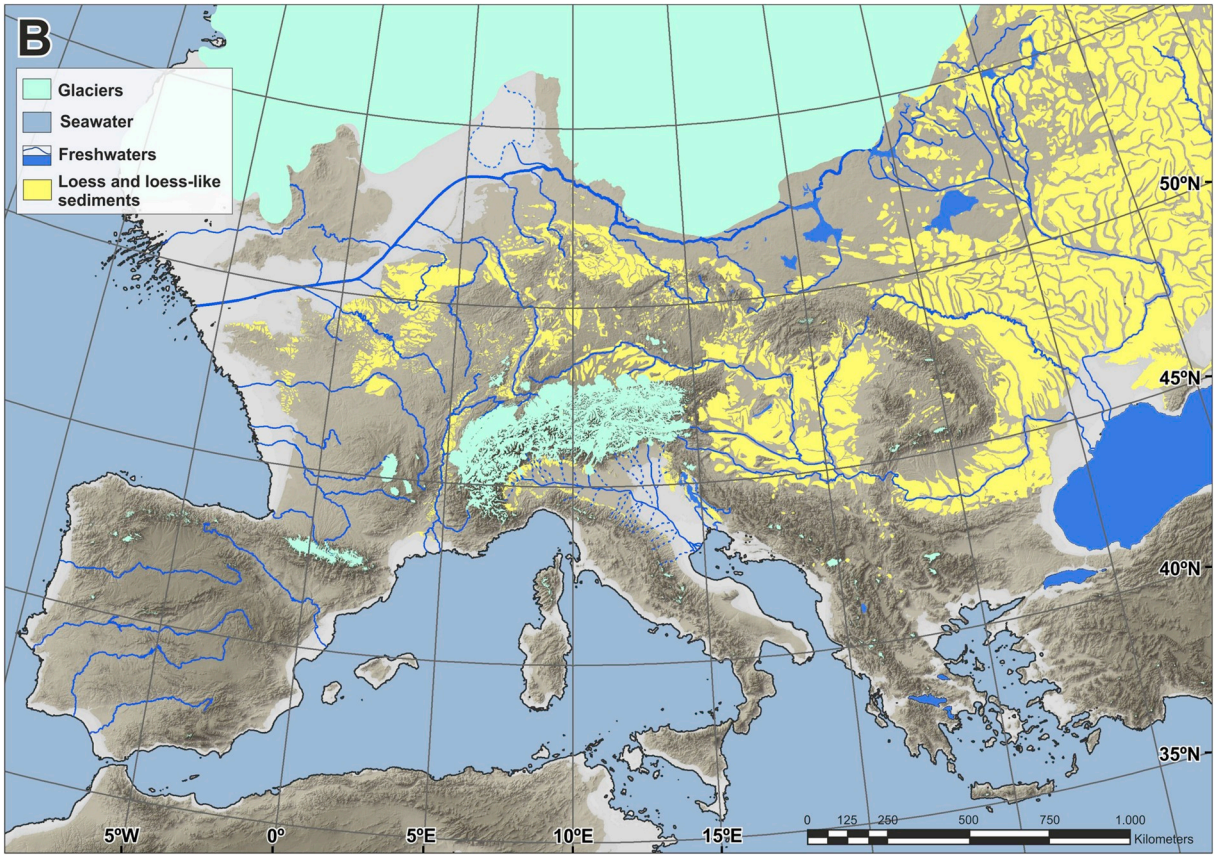

Fig. 4. (*continued*)

4.1.2. Estimating Equilibrium Line Altitudes of mountain glaciers

By using elevational lapse rates we also estimated the Equilibrium Line Altitude (ELA) position during GI 12 in the Central Alps (Vallé et al., unpublished data). Again, temperature differences between the LGM ELA positions (e.g. Kuhlemann et al., 2008; Hughes and Woodward, 2016) and GI 12 were projected over elevational gradients and tested against the temperatures and ELA related to the Egesen stage, Younger Dryas (Kelly et al., 2004; Ivy-Ochs et al., 2008; Delmas, 2015; Ruszkiczay-Rüdiger et al., 2016; Popescu et al., 2017; Gromig et al., 2018). The results of a recent Parallel Ice Sheet Model (PISM) with climate forcing deriving from WorldClim and the ERA-Interim reanalysis (Seguinot et al., 2018) proved to fit our results for the Central Alps (GI 12 ELA 2100 m, 626 m higher than the LGM ELA). As a best approximation, the same value was added to the LGM ELA position for the Pyrenees, Balkans and Carpathians, providing a GI 12 reconstructed ELA of ca. 2400 m, ca. 2100 m and 2000 m, respectively.

4.1.3. The GI 12 palaeoenvironmental map

European vegetation gradients were particularly strong during the major interstadial phases (i.e., spanning about 2000–2500 years), characterized by large arboreal excursions both latitudinally and altitudinally, north and south of the Alps. The GI 12 is one of these key representative warm intervals. In Fig. 4A, we depict the palaeoenvironmental setting of mid and southern Europe (between 52° and 35° latitude N) during GI 12. It is also shown a reconstruction of the coastline: -74 m a.s.l. (Waelbroeck et al., 2002; Antonioli, 2012). A substantial seashore enlargement over Europe led to increased connectivity, especially between the Italian peninsula and the Western Balkans region, between Mediterranean islands, and also the emergence of large areas north of the Black Sea and in the North Sea (Fig. 4A). The Scandinavian Ice Sheet (SIS), which grew during MIS 4, had almost entirely melted at mid MIS 3 (60–45 ka) (Lambeck et al., 2010; Wohlfarth, 2010).

We summarize hereafter the main constrains of the featured eco-climatic zones.

Forest tundra ecozone. The northern timberline was given as the northern limit of the forest tundra mosaic (*sensu* Walter and Breckle, 1986; Holtmeier, 2009; Van Meerbeeck et al., 2011). The abundance of gleysols with charred wood dated to around 45 ka at the base of loess-luvisol sequences in Central and Eastern Europe (Haesaerts et al., 2009; Moine et al., 2017) supports locating the zonoecotone of forest tundra for wetter interstadial phases of MIS 3 between 47° and 52°–54° N, i.e. north of the Alps (Fig. 2A). The geography of northern timberline in Central and Eastern Europe was drawn according to modelling results by Alfano et al. (2003). In the forest tundra zonoecotone, the forest is found mainly in warmer and drier places, with stunted individuals at the waterlogging edaphic ecotone.

Atlantic zone. This biogeographical region closely interacts with the northeast Atlantic Ocean margin. Expansion of Atlantic forests with *Betula, Pinus* and deciduous *Quercus* is recorded during GI 14 and 12, probably reflecting obliquity forcing at higher latitudes (Sánchez Goñi et al., 2008). Vegetation in Western Iberia also responded immediately (within the resolution of the record) to SST changes on millennial time scales during MIS 3. Increases in temperatures offshore translated to increased tree cover on land and vice versa. This rapid response to interstadials warming supports the idea that thermophilous taxa persisted in NW-Iberian refugia throughout the last glacial period (Roucoux et al., 2005).

Iberian region. Average annual precipitation map for the Iberian peninsula (years 1901–2009; Schneider et al., 2014) depicts a strong gradient from the north-western to northern Atlantic coasts (1100–1500 mm/year) to central Spain and Mediterranean areas (250–700 mm/year). During GI 12, humid Atlantic air masses promoted higher moisture availability on the northern coasts of Portugal and Spain, which could support the occurrence of open temperate woodlands. In the inner Iberian areas, grasslands occupied drier lowlands; increasing afforestation was visible along altitudinal gradients.

Adriatic and Tyrrhenian Basins. Lowering of the sea led to the emergence of a wide area north of the 44° parallel in the Adriatic sea. The area hosted terrestrial vegetation, from mixed conifer and broad-leaved woodlands in the inner Friulian-Venetian Plain to more open communities and then grasslands, the latter building a wide belt along the coastal margins. Differences in the humidity regimes between the eastern Adriatic and the western Tyrrhenian Basins bordering Italy are responsible for the asymmetry of ecosystems represented in Fig. 4A. Palaeoecological records from the Tyrrhenian coast suggest almost persistent moisture availability during MIS 3. Similar to the current situation, it can be assumed that precipitation was mainly generated by the orographic uplift of air charged with moisture from the Tyrrhenian Sea.

Balkans and Aegean regions: During GI 12, terrestrial ecosystems were dominated by open temperate woodland and/or temperate forest-steppe south of 40°N, with increasing amount of trees north of this latitude. At lower altitudes, in wider belts bordering the eastern Adriatic, Ionian and eastern Mediterranean Seas, grasslands developed.

Central Anatolian plateau. In the Anatolian region the reconstructed historical GI 12 timberline is located at 1500 m asl. Areas down to 500–800 m could support open forest vegetation, especially along the Turkish coasts of the Black Sea, characterized by a temperate oceanic climate with the greatest amount of precipitation of the whole region (Turkish State Meteorological Service, 2006). Moisture does not reach inland areas; inner plateau bordered by the Pontic Mountains to the north and the Taurus to the south is characterized by a continental climate with strongly contrasting seasons. During GI 12, in these inner areas open grasslands expanded.

A reconstruction of European vegetation patterns during a warm/moist phase of MIS3 was proposed by van Andel and Tzedakis (1998). The vegetation subdivisions provided in this early reconstruction largely overlap with the picture of terrestrial ecosystems provided in our Fig. 4A, with some differences **(i)** the reconstruction of van Andel and Tzedakis (1998) is plotted on a simplified sketch map of Europe not taking into account the altitudinal gradients, indeed represented on our GIS topographic base. This is important as far as temperature and moisture gradients play an important role in determining both latitudinally and altitudinally extents of vegetation belts; **(ii)** minor differences between the two reconstructions are visible in the shape of the limit of the northern timberline (between 53 and 55°N in Fig. 4A - based on Alfano et al., 2003; around 50°N according to van Andel and Tzedakis, 1998); **(iii)** Fig. 4A provides indication on ELA and timberline positions during an interstadial, thanks to data from papers published in recent years and quantitative climate reconstructions for the last glacial cycle.

4.2. Palaeogeography of Southern and Central Europe during LGM

We attempted a LGM palaeogeographical reconstruction of mid-southern Europe in order to allow direct comparison of physical patterns between GI 12 (i.e. a major interstadial within MIS 3) and the subsequent LGM (i.e. 30 to 16.5 ka cal BP, Lambeck et al., 2014) cold phase. For this map, we chose to represent the physical geography of Europe during the time interval spanning both the SIS and the European mountain glacier culminations (26–21 ka cal BP in Europe, see Hughes et al., 2016; Monegato et al., 2017). Interestingly, during this time span, main climatic patterns have been reconstructed through different climate zones according to Köppen-Geiger classification (Becker et al., 2015).

The SIS passed the coast of western Norway at the time of the Laschamp palaeomagnetic excursion (ca. 41 ka) (Valen et al., 1995; Mangerud et al., 2010). At ca. 21 ka the ice-sheet attained its maximum extent (Fig. 4 B; Hughes et al., 2016). During this period the European Alps were extensively covered by an ice-dome which generated valley glaciers. In the Alps, the maximum ice extent was reached during the LGM around 25 ka, when large piedmont glaciers advanced onto the Alpine foreland. This is well constrained by the end-moraine systems, in which the LGM moraines were dated (radiocarbon, OSL and cosmogenic nuclide surface exposure dating methods) and point to large ice lobes at the outlet of major valleys (e.g., Monegato et al., 2007, 2017; Ivy-Ochs et al., 2008, 2018; Ravazzi et al., 2012; Reber et al., 2014; Salcher et al., 2015). In the south-western and in the eastern sectors many valley glaciers remained confined within the valley (e.g., Jorda et al., 2000; Bavec and Verbič, 2011; Rossato et al., 2013, 2018; Federici et al., 2017), as testified by the reconstruction of LGM moraines. In the fringe area of the Alpine chain many isolated small ice caps or mountain glaciers developed without merging with the major trunk glaciers (e.g., Carraro and Sauro, 1979; Forno et al., 2010; Monegato, 2012). Large outwash megafans developed from the front of the Alpine glaciers or from the funnelling of outwash streams in the lower reach of the valleys (Fontana et al., 2014). By this time, large glaciers developed in the Pyrenees and many frontal moraines were dated (Delmas, 2015 and references therein); here glaciers mostly remained confined within the valleys and several small and isolated glaciers occurred (e.g., Pallàs et al., 2010). Other small glacier systems were present in the Iberian mountains; these advances had different age development, from 31 to 20 ka, according to Oliva et al. (2019) compilation. Documented ice-caps in the French Massif Central (de Goer, 1972) and in the Vosges (Seret et al., 1990), but chronology on glacial landforms needs to be improved (Buoncristiani and Campy, 2004).

Valley glaciers spread in the Carpathians and Tatra ranges (e.g., Ehlers et al., 2011; Makos et al., 2018). Their size were reconstructed on the basis of remote sensing and field analyses (Zasadni and Klapyta, 2014) and the age of their maximum spread is constrained with exposure dating at about 25 ka (Engel et al., 2015; Makos et al., 2018).

The Balkan Peninsula was deeply studied in the last decay (see Hughes and Woodward, 2016 for a review). Therein, mountain glaciers developed in a karstic environment with specific characteristics (Adamson et al., 2014; Žebre and Stepišnik, 2015; Žebre et al., 2016). Most of the outwash system into the karstic network and the outwash fans were very confined and limited to the basins where glaciers flowed (Žebre et al., 2016, 2019). Also small glaciers formed on the highest mountain chains of the Apennines (e.g., Giraudi and Giaccio, 2016; Baroni et al., 2018; Mariani et al., 2018).

The region surrounding the Adriatic lowstand plain collected the drainage from Alpine outwash systems and from the surrounding Apennine and Balkan rivers, which had important karst underground flows. The large Adriatic lowstand delta (Fig. 4B; Pellegrini et al., 2017; 2018) accreted as sea level fell down to −120 m or −149 m (Antonioli and Vai, 2004).

Late Pleistocene aeolian sediments are widespread in Europe (e.g. Haase et al., 2007, Fig. 4B) and they represent further indicators of past environmental changes. Loess is commonly distributed in Central, Eastern, and Southern Europe (e.g., Kukla, 1975; Smalley and Leach, 1978; Frechen et al., 1997; Haase et al., 2007; Cremaschi et al., 2015; Marković et al., 2015; Terhorst et al., 2015; Zerboni et al., 2018); in the Mediterranean region loess bodies formed also along the present day coastline (Chiesa et al., 1990; Cremaschi, 1990; Wacha et al., 2011a,b; Boretto et al., 2017). Loess is generally associated with glacial environmental conditions, with dry and cool climate and increased wind strength (Pye, 1995). In continental Europe and in the Mediterranean basin Pleistocene loess accumulated in mid-continental plains free of ice sheets, at the margins of mountain ranges, along the shorelines of the Mediterranean and at the semi-arid margins of the Sahara and Levantine deserts (Obruchev, 1914; Cremaschi, 1990; Haase et al., 2007; Crouvi et al., 2010; Lindner et al., 2017; Lehmkuhl et al., 2018a,b; Zerboni et al., 2018).

In Mediterranean Europe, as in the Po Plain, major loess sources are the outwash plains fed by glaciers flowing from mountains (Alps and Apennines) (Cremaschi, 1990). Loess deposition occurred during most of the Quaternary glacials and was related to a general decrease in forest cover and expansion of semideserts, steppe, and treeless environments (Rousseau et al., 2018). Notwithstanding many efforts in establishing fine MIS 4 to 2 loess chronology with luminescence methods and stratigraphic correlations (e.g., Timar et al., 2010; Timar-Gabor et al., 2011; Thiel et al., 2014) due to intrinsic properties of loess and to the possible occurrence of sedimentary gaps (Thiel et al., 2014), the resolution of loess studies is still lower than those of other continental archives. Likely, Late Pleistocene loess sedimentation occurred, at least, since the end of MIS 4 and during MIS 3 and 2 (Marković et al., 2015; Terhorst et al., 2015). In Italy, loess sedimentation is recorded along the margins of the Po Plain and discontinuously along the shorelines of the Mediterranean, where loess is better preserved within rockshelters (Cremaschi, 2004; Peresani et al., 2008). Italian loess dates back to the Late Pleistocene and mostly formed since the end of MIS 4 (Cremaschi, 1990, 2004); but loess deposits occur as well in sections that contain Mousterian artefacts dating to MIS 3 (e.g., Cremaschi, 1990; Cremaschi et al., 2015; Zerboni et al., 2015; Delpiano et al., 2019). More recently, a few loess bodies have been dated also to MIS 2 (Ferraro, 2009; Zerboni et al., 2015), showing a good continuity in wind sedimentation in the Late Pleistocene, at least at the northern margin of the Po Plain. Italian loess is often interlayered by paleosols, allowing the identification of less arid phases. For instance, at the Val Sorda section a chernozem-like palaeosoil, has been dated at ca. 27 ka BP (Ferraro, 2009); whereas at Monte Netto site moderate pedogenesis (including clay illuviation) compatible with forest cover occurred at times between 44 and 25 ka BP (Zerboni et al., 2015).

5. Focus on spatial vegetation response in Italy during MIS 3

The pie charts presented in Fig. 5 show long-term vegetation dynamics and geographic patterns in Italy between ca. 30 and 60 ka cal BP using data from privileged sites (North to South): Lake Fimon, Lagaccione, Valle di Castiglione and Monticchio. For each record, selected pollen taxa are consistently grouped according to their ecology and climate preferences in order to facilitate their comparison (for further information see caption and legend in Fig. 5).

A higher forest cover in Northern Italy compared to Mediterranean sites is an unchanged background feature during MIS 3. Indeed, the glaciated Alps must have represented a very sharp rainfall boundary leading to almost persistently forested environments in south-eastern alpine foreland and to a northern treeless boreal and continental landscape, as shown by La Grande Pile, Les Echets and Füramoos pollen records (Fig. 2; Woillard, 1978; Beaulieu and Reille, 1984; Guiot et al., 1992; Müller et al., 2003). The palaeoecological record from Lake Fimon documents a mosaic of boreal forests dominated by *Pinus sylvestris/mugo* over the 60 to 30 ka cal BP time period. However, a continuous xerophytic steppe expansion (e.g. *Artemisia* and Chenopodiaceae), coupled with the reduction of temperate elements (deciduous *Quercus* and other thermophilous taxa) in favour of pine woodlands, notably since 40–45 ka, suggests a shift towards drier/colder conditions possibly enhanced by GS 9-HE 4 phase.

The contraction of temperate forests is also recorded throughout MIS 3 in central Italy (Lagaccione and Valle di Castiglione) and southern Italy at Lago Grande di Monticchio. In these sites, open forests dominated by deciduous *Quercus*, *Corylus, Fagus, Tilia, Ulmus* and *Carpinus betulus* experienced their maximum expansion between ca. 60–45 ka. Afterwards, open environments (*Artemisia*-dominated steppe/wooded steppe) expanded between 45 and 30 ka (Fig. 5).

This general overview suggests latitudinal (and also altitudinal) climatic patterns and rainfall gradients along the Italian peninsula due to its complex physiographic structure (i.e. the presence of two high mountain ranges, Alps and Apennines), to be taken into account when reconstructing past vegetation dynamics as it has already been shown for Greece (Tzedakis et al., 2004).

6. Archaeological framework

During the first half of MIS 3, and particularly during GIs 14/13 ca. 55–48 ka, natural environments were favourable for AMHs to migrate from Africa into Europe (Müller et al., 2011). The scenario of an initial AMHs movement into Europe is supported by industries associated with modern hominin remains found in few excavated localities: Üçağızlı cave (Turkey) (Güleç et al., 2002; Kuhn et al., 2009); Ksar Akil (Lebanon) (Copeland and Yazbeck, 2002; Yazbeck, 2004; Douka et al., 2013); Manot cave (Israel) (Hershkovitz et al., 2015). Around 45 to 39 ka, Neandertals were replaced by AMHs (Higham et al., 2014), and a variety of early Upper Palaeolithic cultures emerged (e.g., Uluzzian and Proto-Aurignacian in the central-eastern Mediterranean regions; see Arrighi et al.,this issue and Marciani et al., this issue).

The cultural complex known as Uluzzian has been attested in the Italian Peninsula and southern Balkans around 45–40 ka (Fig. 6; Palma di Cesnola, 1989; Ronchitelli et al., 2009; Moroni et al., 2013; Peresani, 2014; Zanchetta et al., 2018). This techno-complex was coeval with the arrival of AMHs in Europe as evidenced by the anatomical features of two deciduous teeth discovered in Grotta del Cavallo in Apulia (Benazzi et al., 2011, although challenged by Zilhão et al., 2015, and further discussed in Moroni et al., 2018). Along the Italian Peninsula, the Uluzzian is currently best known in cave sedimentary successions by its stratigraphic position above the Mousterian and under the Proto-Aurignacian, when the latter is present, and also in several open-air sites (Fig. 6). Recently, the Uluzzian has also been observed in northern Italian cave sites, expanding its cultural borders from what was thought to be exclusively central-southern after the discovery of assemblages at Grotta Fumane and at the Riparo Broion shelter (Peresani et al., 2008, 2016, 2018). Other sites in the Adriatic-Ionian region exhibit Uluzzian elements (Crvena Stijena; Mihailović and Whallon, 2017; Klissoura Cave; Starkovich, 2017; Kephalari; Darlas and Psathi, 2016), opening new perspectives in looking at the appearance and spread of the Uluzzian over the entire area of the Adriatic basin.

In several sites, the Middle to Upper Palaeolithic transition is documented by the Proto-Aurignacian technocomplex. The available chronological framework indicates a Proto-Aurignacian occupation ending with the Campanian Ignimbrite eruption in Southern Italian Castelcivita (Gambassini, 1997) and Serino sites (Lowe et al., 2012; Wood et al., 2012). However, this tephrostratigraphic marker also constrains the end of the Uluzzian techno-complexes at Grotta del Cavallo on the Ionic coast of Salento (Lecce) (Zanchetta et al., 2018, section 7.2). In N-W Italy, the earliest Proto-Aurignacian is that of the Balzi Rossi sites complex in the region of Liguria (NW Italy), where it has been identified at Riparo Mochi and Riparo Bombrini sites (Douka et al., 2012; Riel-Salvatore and Negrino, 2018). At these sites, the main outlines of the industry remain stable beyond the end of GS9/HE4 (Riel-Salvatore and Negrino, 2018), comparably to Grotta Fumane in the north of Italy (Falcucci et al., 2017; Falcucci and Peresani, 2018). The assessment of these temporal-spatial issues and new chronological information are fundamental for understanding the dynamics of the cultural and ecological-anthropological changes that occurred in S-Europe at the Middle to Upper Palaeolithic transition.

Already before 43 ka, very early Aurignacian assemblages, reflecting an initial AMHs advance into central Europe, have also been found along the Danube (Willendorf II, Lower Austria; Nigst et al., 2014), suggesting the Danube's role as a spatial corridor for human dispersal in the Early Upper Palaeolithic (e.g., Floss, 2003; Hussain and Floss, 2016). A similar role is hypothesized for the Don River system near the Black Sea (Anikovich et al., 2007). Beside large river systems, also coastal plains played a relevant role channelling AMHs dispersal into Europe (Mellars, 2006; Hublin, 2014). The close similarity between the available dates for the early AMH arrival in the Mediterranean and in Germany on the Danube, might suggest a rapid access in Europe via two routes, along both the Danube corridor and the Mediterranean coasts (Douka et al., 2012).

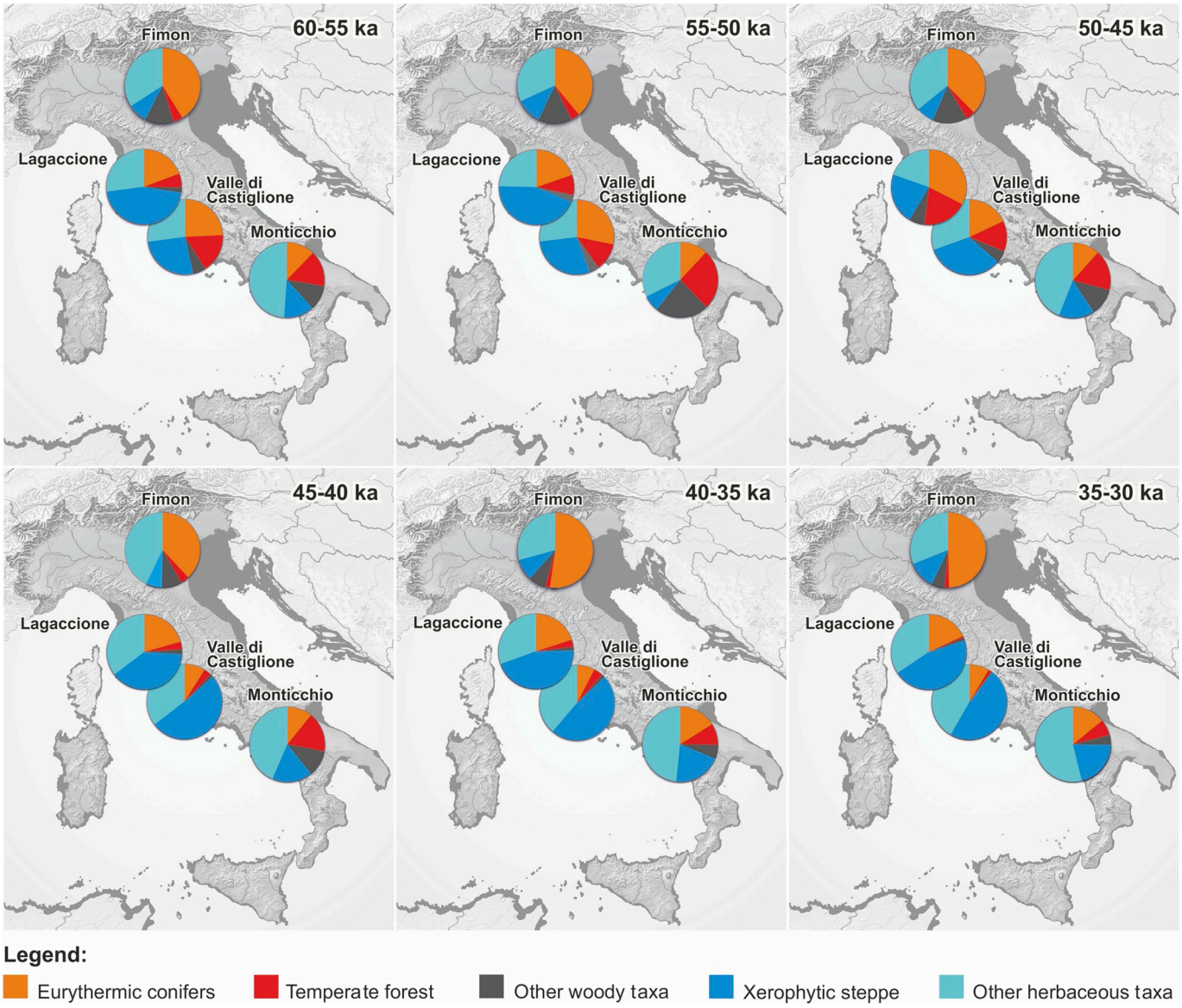

Fig. 5. Spatial vegetation changes at fixed 5 ka yrs long time slices between 60 and 30 ka yrs cal BP. The selected taxa are grouped according to their ecology and climatic preferences. Eurythermic conifers (orange): sum of *Pinus* and *Juniperus*; Temperate forest (red): sum of deciduous *Quercus*, *Alnus*, *Fagus*, *Acer*, *Corylus*, *Carpinus*, *Fraxinus*, *Ulmus*, *Tilia* and *Salix*; Xerophytic taxa (dark blue): sum of *Artemisia* and Chenopodiaceae. Italian Peninsula sketch map shows sea level 70 m below the present-day coastline (courtesy by S. Ricci, University of Siena), based on the global sea-level curve by Waelbroeck et al. (2002), but lacking estimation of post-MIS3 sedimentary thickness and eustatic magnitude. (For interpretation of the references to colour in this figure legend, the reader is referred to the Web version of this article.)

7. Chronological issues

7.1. Difficulties in dating the Middle to Upper Palaeolithic transition

Building reliable radiocarbon chronologies for sequences covering time intervals beyond and/or close to the limit of the radiocarbon technique (i.e., ca. 50 ka) remain challenging. Indeed, the low levels of residual ^{14}C activity induces lower precision (higher uncertainty) and accuracy (higher offset of the measured isotope ratio with respect to the actual one) of AMS measurements and makes samples much more vulnerable to contamination (e.g., Bird et al., 1999; Higham, 2011; Wood, 2015). In old samples, due to the low ^{14}C content, even very negligible percentages of modern carbon give very high contamination levels leading to wholly distorted chronologies, with resulting ages that can be younger of several millennia (Higham et al., 2009; Higham, 2011). Indeed, this makes the dating of small amounts of ancient carbon, i.e., more prone to contamination, even more challenging (e.g., Bird et al., 2014). Such problems can be partially overcome in long, continuous sedimentary succession that are biostratigraphically well-constrained using indirect approaches based on record alignment strategies, i.e., one record on a depth-scale is aligned onto a "dated reference" record (Govin et al., 2015); provided that the underlying assumptions, i.e., recognition of the events and their one-to-one correlation, are reasonably demonstrated. Yet, whenever possible, tephra markers and/or relative chronologies based on varved sediments can also be used to refine or validate age-models.

7.2. The Campanian Ignimbrite (CI) marker

The Campanian Ignimbrite (CI) super-eruption (southern Italy, $^{40}Ar/^{39}Ar$ age: 39.85 ± 0.14 ka, 2σ; ^{14}C age: 34.29 ± 0.09 ^{14}C ka BP, 1σ; Giaccio et al., 2017) produced the most widespread tephra of western Eurasia, extending from the Tyrrhenian Sea to the Russian Plain (e.g., Costa et al., 2012; Marti et al., 2016, Fig. 7). Its relevance as a key chronological

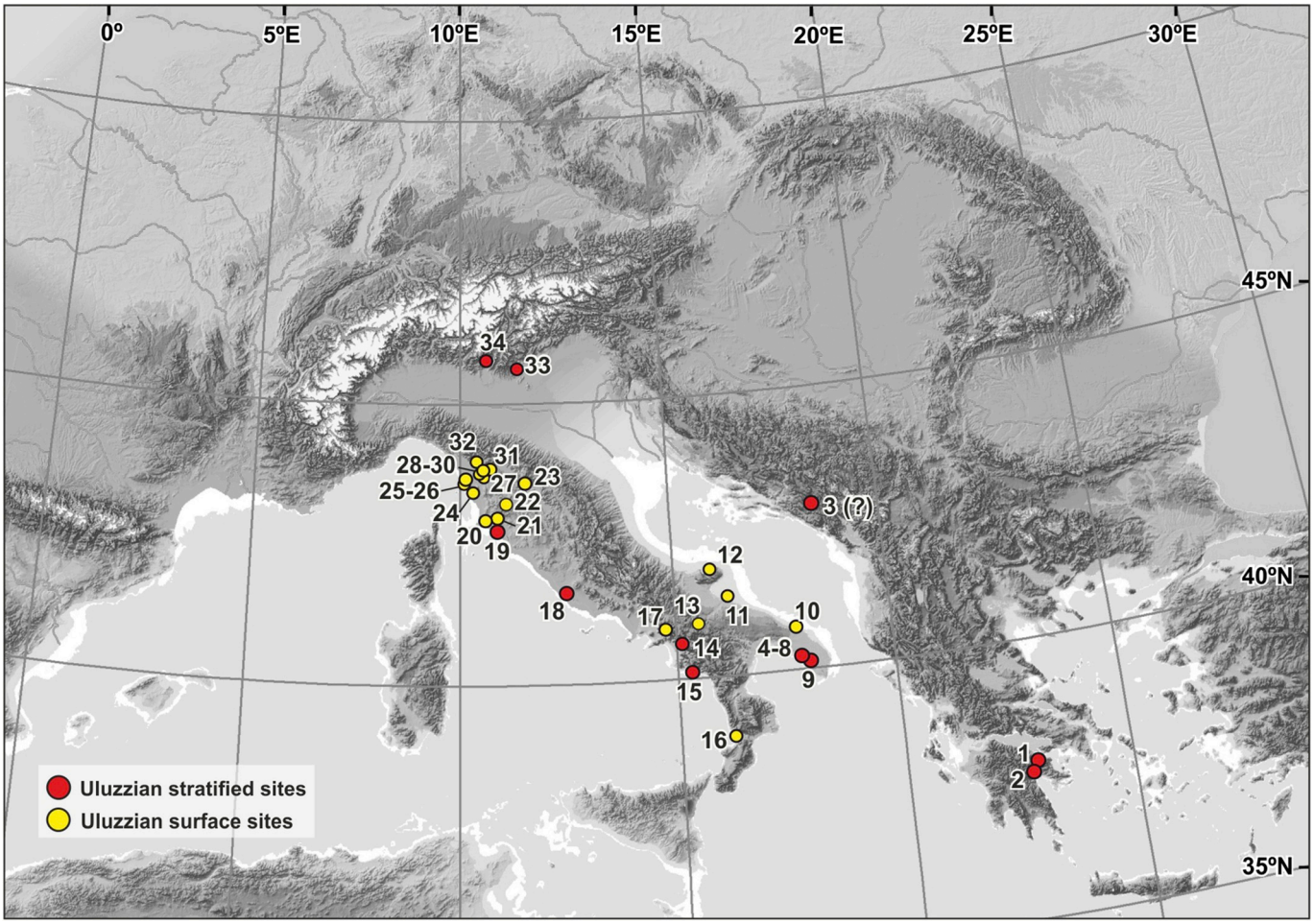

Fig. 6. Sketch map showing the position of the Palaeolithic sites documenting the Uluzzian culture: 1) Klissoura Cave (Stiner et al., 2007); 2) Kephalari Cave (Darlas and Psathi, 2016); 3) Crvena Stijena (Morley and Woodward, 2011); 4) Grotta del Cavallo (Moroni et al., 2018); 5) Grotta di Serra Cicora (Spennato, 1981); 6) Grotta Mario Bernardini (Borzatti von Löwenstern, 1970); 7) Grotta di Uluzzo (Borzatti von Löwenstern, 1965); 8) Grotta di Uluzzo C (Borzatti von Löwenstern, 1966); 9) Grotta delle Veneri (Cremonesi, 1987); 10) Torre Testa (Moroni et al., 2018); 11) Falce del Viaggio (Moroni et al., 2018); 12) Foresta Umbra (Moroni et al., 2018); 13) Atella Basin (Moroni et al., 2018); 14) Castelcivita (Gambassini, 1997); 15) Grotta della Cala (Benini et al., 1997); 16) S. Pietro a Maida (Moroni et al., 2018); 17) Tornola (Moroni et al., 2018); 18) Colle Rotondo (Moroni et al., 2018); 19) Grotta della Fabbrica (Dini and Tozzi, 2012); 20) Val Berretta (Moroni et al., 2018); 21) Poggio Calvello (Moroni et al., 2018); 22) S. Lucia I (Moroni et al., 2018); 23) Indicatore (Moroni et al., 2018); 24) Villa Ladronaia (Moroni et al., 2018); 25) Maroccone (Moroni et al., 2018); 26) Salviano (Moroni et al., 2018); 27) Podere Collina (Moroni et al., 2018); 28) Val di Cava (Moroni et al., 2018); 29) Casa ai Pini (Moroni et al., 2018); 30) San Romano (Moroni et al., 2018); 31) San Leonardo (Moroni et al., 2018); 32) Porcari (Moroni et al., 2018); 33) Riparo del Broion (Peresani et al., 2019); 34) Grotta Fumane (Peresani et al., 2016).

and stratigraphic marker for addressing a series of issues concerning the European MIS 3 period – including the tempo and the palaeoecological factors involved in the human bio-cultural evolution at the Middle to Upper Palaeolithic transition – has been recognised long ago (e.g., Fedele et al., 2003) and eventually consolidated by a number of papers: e.g., Giaccio et al. (2006) (see Higham et al., 2009 for the updated chronology of Grotta Fumane); Pyle et al. (2006); Fedele et al. (2008); Giaccio et al. (2008); Hoffecker et al. (2008); Lowe et al. (2012); Satow et al. (2015); Wutke et al. (2015); Wulf et al. (2018); Zanchetta et al. (2018).

At several archaeological sites of the central Mediterranean, Balkans and Russian Plain the CI tephra acts as a marker for the end of either final Mousterian with Uluzzian elements (Crvena Stijena, Montenegro, Morley and Woodward, 2011; Mihailović and Whallon, 2017), Uluzzian (Apulia region in southern-eastern Italy and Greece; e.g., Douka et al., 2014; Zanchetta et al., 2018) or Proto-Aurignacian techocomplexes (e.g., Serino open-air site and Castelcivita Cave in southern-western Italy and Kostenki site complex in Russia; e.g., Giaccio et al., 2008 and references therein). However, although falling in its dispersal area, the CI has not been detected at the Adriatic site of Grotta Paglicci (Apulia, Southern Italy) and on the opposite Tyrrhenian side, at Grotta della Cala. In both caves the Protoaurignacian seems to stretch beyond the CI event based on ^{14}C chronology (Paglicci) and the studied materials (Marciani et al., this issue).

The CI tephra occurs in the above-mentioned sites either as a relatively proximal, thick primary pyroclastic succession (e.g., Serino open-air site; Accorsi et al., 1978; Giaccio et al., 2006) or as a discrete layer, with a sharp lower contact with underling sediments, made of purely volcanic material (i.e., glass shards or pumice fragments with mineral accessories) with no or negligible contamination by clastic sediments. These features are consistent with a sub-primary (re)deposition of ash layers by the wind or run-off shortly after its emplacement as primary fallout along landforms nearby sheltered or open-air archaeological sites (e.g., Bruins et al., 2019). Specifically, at Castelcivita site, both Plinian pumice and co-ignimbritic ash layers are recorded in their eruptive stratigraphic order, suggesting that the two eruptive units were transported and redeposited in the cave immediately after their fall (fall and rolling process) (Giaccio et al., 2008; Giaccio et al., 2006). The sub-primary nature of the CI tephra, i.e., no appreciable time elapsed between CI tephra deposition and the eruption, is also supported by the available radiocarbon chronology of the archaeological layers immediately below CI tephra strata, which are statistically

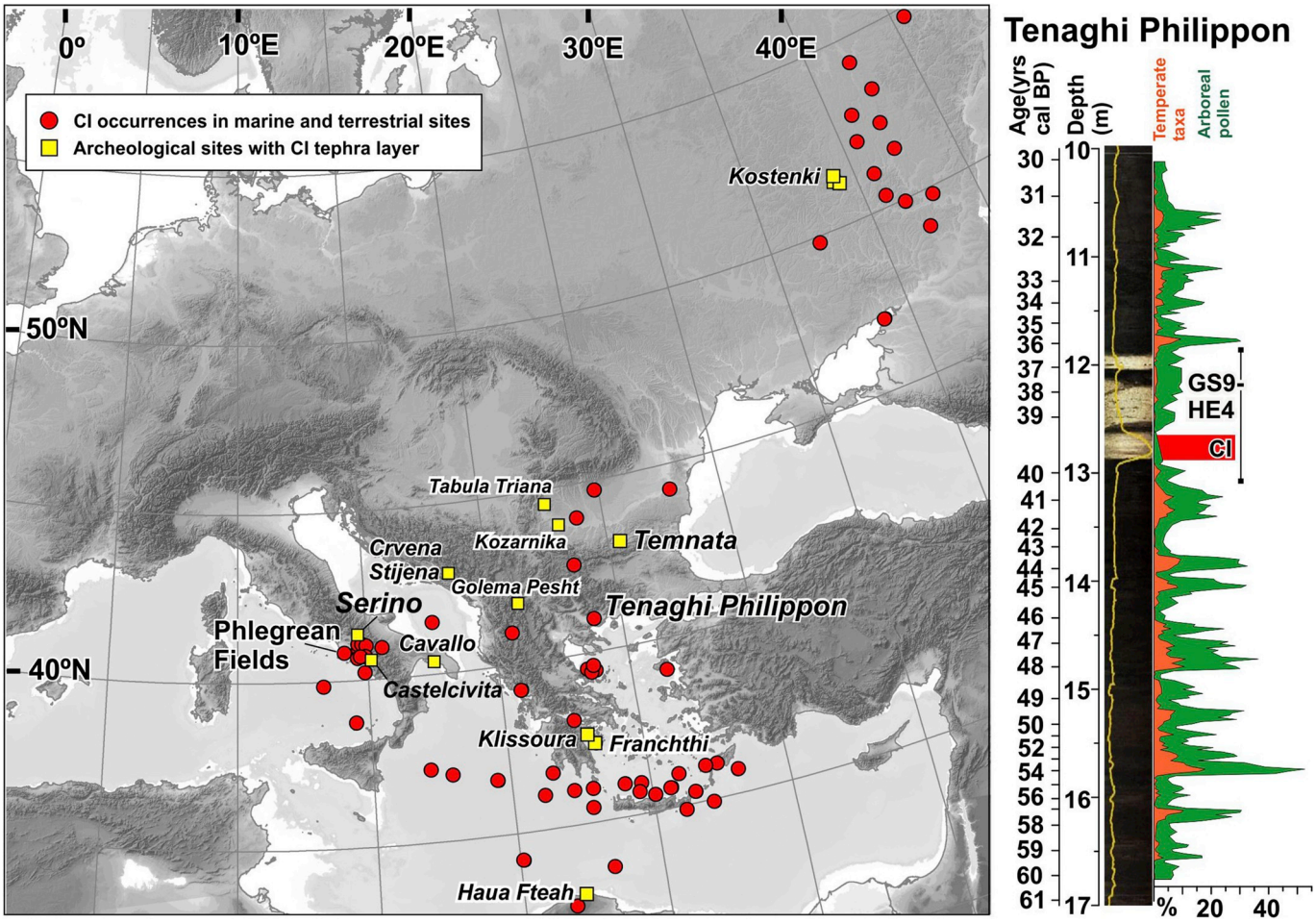

Fig. 7. Geographic distribution of the Campanian Ignimbrite (CI) distal tephra layer in terrestrial and marine records (red dots) and archaeological sites (yellow squares). On the right: Tenaghi Philippon paleoecological record showing the CI chronostratigraphic position. Selected pollen curves of % arboreal pollen (green) and temperate taxa (orange) between 30 and 60 ka are shown. (For interpretation of the references to colour in this figure legend, the reader is referred to the Web version of this article.)

indistinguishable from the CI eruption age (Benazzi et al., 2011; Wood et al., 2012; Douka et al., 2014; Giaccio et al., 2017). On the whole, both radiocarbon chronology and CI tephra marker suggest that around 40 ka the central Mediterranean region was a cultural, and possibly biological, mosaic, suggesting the possible coeval occurrence of the final Mousterian (Crvena Stijena), Uluzzian (Apulia and Greece) and Protaurignacian lithic technocomplexes (Campania).

Particularly significant is also the climatostratigraphic position of the CI tephra as revealed by a number of marine and terrestrial palaeoclimatic records spread in the wide region of its dispersal area (Fig. 7). In this framework, the palaeoecological and tephrostratigraphic high-resolution (120 yr/sample) record of Tenaghi Philippon (Greece, Wulf et., al 2018) offers the unique opportunity to compare the chronostratigraphic position of CI in relation to the palaeoenvironmental context at a centennial scale during the Middle to Upper Palaeolithic transition. In detail, CI deposition occurred ca. 1000 years after the onset of a phase of marked arboreal pollen drop corresponding to the GS 9 (ca. 40.58 cal ka BP) and 3280 years before the onset of GI8 (ca. 36.3 cal ka BP) (Fig. 7; Wulf et al., 2018). Similarly, at Monticchio site, the CI was deposited ca. 820 years after the onset of GS 9 (Fig. 3). However, at Tenaghi Philippon the resulting total duration of ca. 4280 years for GS 9 strongly deviates from the ca. 2000 years obtained at Lago Grande di Monticchio (Wutke et al., 2015) and from the 1680 years in the NGRIP record (i.e. from 39.90 to 38.22 ka GICC05; Rasmussen et al., 2014). A similar position is verified in number of other terrestrial and marine palaeoenvironmental records (e.g., Mediterranean and Black Sea marine records and Lake Ohrid, and Lesvos Island pollen profiles; see Giaccio et al., 2017 and references therein). Despite the general agreement in placing the CI well after the beginning of GS 9 (ca. 400 years, according to the alignment of records proposed in Giaccio et al., 2017), which is marked by a drop in arboreal pollen and temperate taxa (Fig. 7), it seems that further investigations are needed to fully disentangle temporal discrepancies between records and to convincingly correlate the interval encompassing GI 8–10 to the D-O events. This is also challenging due to the inadequate resolution of most of the available pollen records if compared to the short GI 9 duration (i.e., 250-yr-long GICC05; Rasmussen et al., 2014), which only briefly interrupts the GS 10 to GS 9 interval representing over 4 millennia of cold stadial conditions.

With specific regards to these chronological issues, it is worth noting that the paired, high-precision, multiple $^{40}Ar/^{39}Ar$ and ^{14}C ages for the CI revealed an offset of ca. 1 ka between the calendar age of the CI as determined by its direct $^{40}Ar/^{39}Ar$ dating and the calibrated ^{14}C age of the CI using IntCal13 calibration curve (Giaccio et al., 2017), thus highlighting the occurrence of a further source of uncertainty when comparing records whose age models are based on calibrated ^{14}C ages with others anchored to different time-scales (e.g., U/Th or Greenland ice chronology). This offset is now confirmed by a recent study, which reports a record of paired U/Th and ^{14}C ages from the Chinese Hulu Cave stalagmite, continuously spanning the last 54 ka (Cheng et al., 2018). This new record also reveals a radiocarbon plateau between ca. 37.5 ka and ca. 39.1 ka at ca. 33.5 ^{14}C ka BP that could have affected the age model of records based on ^{14}C chronology and thus be responsible for the above-mentioned notable age discrepancy in the

length of the GS9 as recorded in different Mediterranean records. A distortion of the IntCal13 calibration curve at this time interval is also suggested by the recently published continuous record of the $\Delta^{14}C$ spanning between ca. 47.3 and 39.6 ka cal. BP from the Tenaghi Philippon lake succession (Staff et al., 2019).

All this information strictly related to this stratigraphic marker consolidate the notion of the CI as a pivotal tool for deciphering and evaluating the potential interconnection between climate, environmental, and human biological-cultural dynamics at the Middle to Upper Palaeolithic transition, as well as in disentangling several temporal-spatial issues, crucial for understanding the mechanisms underlying the interaction between AMHs and Neandertals.

8. Concluding remarks and future developments

In this review, we summarized the current state of knowledge, also contributing with new elaborations of available data, on climate history, terrestrial ecosystems and palaeogeography, with the main aim to place Neanderthals and AMHs in the context of MIS 3 European landscape. Neanderthals lived in Eurasia alongside anatomically modern humans until ca. 40 ka. This overlap suggests direct or indirect contacts between the two species on a European sub-continental scale, potentially leading to interbreeding and cultural exchanges (Higham et al., 2014). To decipher the possible implications of climate variability and palaeoenvironmental transformation in such human processes, including Neanderthals extinction, two main aspects must be kept in mind: (i) the millennial/sub-millennial terrestrial response to high-frequency climate variability resulted in a pronounced and rapid alternation between forested and more open environments. Interestingly, the most relevant tree cover reductions in southern Europe are correlated to HEs, notably GS9-HE4 (ii) a long-term climatic trend (i.e., between ca. 50 and 25 ka); that led to dramatic increasing of the glaciers extent and lowering of the sea level, with major impacts on the coast landscape and on physiography and vegetation patterns. This implied the progressive development of effective ecological and physiographic barriers (i.e. the Alpine ice-dome) that limited connections between continental and Mediterranean Europe. In contrast, the gradual enlargement of coastlines and reorganization of European river systems may have played a key role in the migration processes.

To better understand and integrate these aspects, within the ERC - SUCCESS project, a Work Package is specifically dedicated. Studies will concentrate on the time span between Heinrich Event 5 to 3, known for their strong impact in Mediterranean Europe, the Balkans and Italy (Follieri et al., 1988; Allen et al., 2000; Lézine et al., 2010; Pini et al., 2010; Müller et al., 2011; Panagiotopoulos et al., 2014).

Attention will be paid to the reference record of Lake Fimon (Venetian Alpine foothills, north-eastern Italy). This area is indeed well-known as it provides both a Late Pleistocene palaeoecological record (Pini et al., 2010) and several Middle to Late Palaeolithic sites yielding evidence of Neandertal and AMH occupation (Grotta Fumane and Riparo Broion shelter; Peresani, 2011, Fig. 6). High-resolution palynostratigraphic researches currently in progress on the Lake Fimon core will be matched with archaeological information from cave deposits in the same region to answer specific questions relevant to the ERC Project, i.e. the effects of climate variability on the environments of last Neandertals - early AMH, the role of fire, etc. Finally, to better comprehend regional vegetation patterns and eco-climatic gradients across the Italian peninsula, palaeoenvironmental proxies from Lake Fimon will be profitably compared to Central and Southern Italian records, through the elaboration of available series and the investigation of new sites.

Acknowledgements

This work was funded by ERC under the European Union's Horizon 2020 research and innovation programme (grant agreement No 724046 - SUCCESS); website: http://www.erc-success.eu/. Thanks are due to Prof. D. Haase, who kindly provided the shapefiles of loess distribution in Europe used in Fig. 4 B and to Prof. P.C. Tzedakis for helpful comments on Fig. 4 A. We also thank three anonymous reviewers and the editor Dusan Boric for the valuable comments, which improved the quality of the manuscript.

References

Accorsi, C.A., Aiello, E., Bartolini, C., Castelletti, l., Rodolfi, G., Ronchitelli, A., 1978. Il giacimento paleolitico di Serino (Avellino): stratigrafia, ambienti e paletnologia. Atti della Società Toscana di Scienze Naturali 86 (1979), 435–487.

Adamson, K.R., Woodward, J.C., Hughes, P.D., 2014. Glaciers and rivers: Pleistocene uncoupling in a Mediterranean mountain karst. Quat. Sci. Rev. 94, 28–43.

Alfano, M.J., Barron, E.J., Pollard, D., Huntley, B., Allen, J.R.M., 2003. Comparison of climate model results with European vegetation and permafrost during oxygen isotope stage three. Quat. Res. 59, 97–107.

Allen, J.R.M., Brandt, U., Brauer, A., Hubberten, H.-W., Huntley, B., Keller, J., Kraml, M., Mackensen, A., Mingram, J., Negendank, J.F.W., Nowaczyk, N.R., Oberhänsli, H., Watts, W.A., Wulf, S., Zolitschka, B., 1999. Rapid environmental changes in southern Europe during the last glacial period. Nature 400, 740–743.

Allen, J.R.M., Watts, W.A., Huntley, B., 2000. Weichselian palynostratigraphy, palaeovegetation and palaeoenvironments; the record from Lago Grande di Monticchio, southern Italy. Quat. Int. 73/74, 91–110.

Alvarez-Solas, J., Charbit, S., Ritz, C., Paillard, D., Ramstein, G., Dumas, C., 2010. Links between ocean temperature and iceberg discharge during Heinrich events. Nat. Geosci. 3, 122–126.

Alvarez-Solas, J., Robinson, A., Montoya, M., Ritz, C., 2013. Iceberg discharges of the last glacial period driven by oceanic circulation changes. Proc. Natl. Acad. Sci. 110 (41), 16350–16354.

Andersen, K.K., Svensson, A., Johnsen, S.J., Rasmussen, S.O., Bigler, M., Röthlisberger, R., Ruth, U., Siggaard-Andersen, M.L., Steffensen, J.P., Dahl-Jensen, D., Vinther, B.M., Clausen, H.B., 2006. The Greenland Ice Core chronology 2005, 15–42 kyr. Part 1: constructing the time scale. Quat. Sci. Rev. 25, 3246–3257.

Andrews, J.T., Voelker, A.H., 2018. "Heinrich events" (& sediments): a history of terminology and recommendations for future usage. Quat. Sci. Rev. 187, 31–40.

Anikovich, M.V., Sinitsyn, A.A., Hoffecker, J.F., Holliday, V.T., Popov, V.V., Lisitsyn, S.N., Forman, S.L., Levkovskaya, G.M., Pospelova, G.A., Kuz'mina, I.E., Burova, N.D., Goldberg, P., Macphail, R.I., Giaccio, B., Praslov, N.D., 2007. Early upper Paleolithic in eastern Europe and implications for the dispersal of modern humans. Science 315 (5809), 223–226.

Antonioli, F., 2012. Sea level change in western-central Mediterranean since 300 kyr: comparing global sea level curves with observed data. Alpine and Mediterranean Quaternary 25 (1), 15–23.

Antonioli, F., Vai, G.B., 2004. Litho-palaeoenvironmental Maps of Italy during the Last Two Climatic Extremes. Climex Maps Italy e Explanatory Notes, Bologna, pp. 80.

Archibold, O.W., 2012. Ecology of World Vegetation. Springer Science & Business Media.

Arrighi, S., Moroni, A., Tassoni, L., Boschin, F., Badino, F., Bortolini, E., Boscato, P., Crezzini, J., Figus, C., Forte, M., Lugli F., Marciani, G., Oxilia G., Negrino F., Riel-Salvatore J., Romandini, M., Spinapolice, E. E., Peresani, M., Ronchitelli, A., Benazzi, S., this issue. Bone Tools, Ornaments and Other Unusual Objects during the Middle to Upper Palaeolithic Transition in Italy.

Bagniewski, W., Meissner, K.J., Menviel, L., 2017. Exploring the oxygen isotope fingerprint of Dansgaard-Oeschger variability and Heinrich events. Quat. Sci. Rev. 159, 1–14.

Bar-Matthews, M., Ayalon, A., Kaufman, A., Wasserburg, G.J., 1999. The Eastern Mediterranean paleoclimate as a reflection of regional events: Soreq cave, Israel. Earth Planet. Sci. Lett. 166 (1–2), 85–95.

Bar-Matthews, M., Avalon, A., Kaufman, A., 2000. Timing and hydrological conditions of sapropel events in the Eastern Mediterranean as evident from speleothems, Soreq cave, Israel. Chem. Geol. 169 (1–2), 145–156.

Bard, E., Rostek, F., Turon, J.L., Gendreau, S., 2000. Hydrological impact of Heinrich events in the subtropical northeast Atlantic. Science 289 (5483), 1321–1324.

Barker, S., Chen, J., Gong, X., Jonkers, L., Knorr, G., Thornalley, D., 2015. Icebergs not the trigger for North Atlantic cold events. Nature 520, 333–336.

Baroni, C., Guidobaldi, G., Salvatore, M.C., Christl, M., Ivy-Ochs, S., 2018. Last glacial maximum glaciers in the Northern Apennines reflect primarily the influence of southerly storm-tracks in the western Mediterranean. Quat. Sci. Rev. 197, 352–367.

Bartolomei, G., Broglio, A., Cattani, L., Cremaschi, M., Lanzinger, M., Leonardi, P., 1987-88. Nuove ricerche nel deposito pleistocenico della Grotta di Paina sui Colli Berici (Vicenza). Atti Istituto Veneto SS.LL.AA. CXLVI. pp. 112–160.

Bavec, M., Verbič, T., 2011. Glacial history of Slovenia. Dev. Quat. Sci. 15, 385–392.

de Beaulieu, J.-L., Reille, M., 1984. A long upper Pleistocene pollen record from Les Echets, near Lyon. Boreas 1, 111–132.

de Beaulieu, J.-L., Reille, M., 1992a. The last climatic cycle at La Grand Pile (Vosges, France). A new pollen profile. Quat. Sci. Rev. 11, 431–438.

de Beaulieu, J.-L., Reille, M., 1992b. Long Pleistocene sequences from the Velay plateau (Massif central, France). I. Ribains maar. Veg. Hist. Archaeobotany 1, 233–242.

Becker, D., Verheul, J., Zickel, M., Willmes, C., 2015. LGM Paleoenvironment of Europe – Map. CRC806-Database. https://doi.org/10.5880/SFB806.15.

Been, E., Hovers, E., Ekshtain, R., Malinsky-Buller, A., Agha, N., Barash, A., Bar-Yosef Mayer, D.E., Benazzi, S., Hublin, J.-J., Levin, L., Greenbaum, N., Mitki, N., Oxilia, G., Porat, N., Roskin, J., Soudack, M., Yeshurun, R., Shahack-Gross, R., Nir, N.,

Stahlschmidt, M.C., Rak, Y., Barzilai, O., 2017. The first Neanderthal remains from an open-air Middle Palaeolithic site in the Levant. Sci. Rep. 7, 2958.
Benazzi, S., Douka, K., Fornai, C., Bauer, C.C., Kullmer, O., Svoboda, J., Pap, I., Mallegni, F., Bayle, P., Coquerelle, M., Condemi, S., Ronchitelli, A., Harvati, K., Weber, G.W., 2011. Early dispersal of modern humans in Europe and implications for Neanderthal behaviour. Nature 479, 525–528.
Benazzi, S., Slon, S., Talamo, S., Negrino, F., Peresani, M., Bailey, S.E., Sawyer, S., Panetta, D., Vicino, G., Starnini, E., Mannino, M.A., Salvadori, P.A., Meyer, M., Pääbo, S., Hublin, J.-J., 2015. The makers of the Protoaurignacian and implications for Neandertal extinction. Science 348, 793–796.
Benini, A., Boscato, P., Gambassini, P., 1997. Grotta della Cala (Salerno): industrie litiche e faune uluzziane e aurignaziane. Rivista di Scienze Preistoriche 48, 37–95.
Bird, M.I., Ayliffe, L.K., Fifield, L.K., Turney, C.S.M., Cresswell, R.G., Barrows, T.T., David, B., 1999. Radiocarbon dating of "old" charcoal using a wet oxidation, stepped-combustion procedure. Radiocarbon 41 (2), 127–140.
Bird, M.I., Levchenko, V., Ascough, P.L., Meredith, W., Wurster, C.M., Williams, A., Tilston, E.L., Snape, C.E., Apperley, D.C., 2014. The efficiency of charcoal decontamination for radiocarbon dating by three pre-treatments–ABOX, ABA and hypy. Quat. Geochronol. 22, 25–32.
Blockley, S.P.E., Lane, C.S., Hardiman, M., Rasmussen, S.O., Seierstad, I.K., Steffensen, J.P., Svensson, A., Lotter, A.F., Turney, C.S.M., Bronk Ramsey, C., 2012. Synchronisation of palaeoenvironmental records over the last 60,000 years, and an extended INTIMATE event stratigraphy to 48,000 b2k. Quat. Sci. Rev. 36, 2–10.
Bond, G., Heinrich, H., Broecker, W., Labeyrie, L., McManus, J., Andrews, J., Huon, S., Jantschik, R., Clasen, S., Simet, C., Tedesco, K., Klas, M., Bonani, G., Ivy, S., 1992. Evidence for massive discharges of icebergs into the North Atlantic ocean during the last glacial period. Nature 360, 245–249.
Bond, G., Broecher, W., Johnsen, S.J., MacManus, J., Laberie, L., Jouzel, J., Bonani, G., 1993. Correlations between climate records from North Atlantic sediments and Greenland ice. Nature 365, 143–147.
Boretto, G., Zanchetta, G., Ciulli, L., Bini, M., Fallick, E., Lezzerini, M., Colonese, A.C., Zembo, I., Trombino, L., Regattieri, E., Sarti, G., 2017. The loess deposits of Buca dei Corvi section (Central Italy): revisited. Catena 151, 225–237.
Borzatti von Löwenstern, E., 1965. La grotta di Uluzzo (campagna di scavi 1964). Rivista di Scienze Preistoriche 19, 41–52.
Borzatti von Löwenstern, E., 1966. Alcuni aspetti del Musteriano nel Salento. (La grotta-riparo di Torre dell'Alto e la grotta di Uluzzo C). Scavi 1965 e 1966. Rivista di Scienze Preistoriche 21, 203–287.
Borzatti von Löwenstern, E., 1970. Prima campagna di scavi nella grotta "Mario Bernardini" (Nardò - Lecce). Rivista di Scienze Preistoriche 25, 89–125.
Broecker, W.S.T., Peng, H., Jouzel, J., Russell, G., 1990. The magnitude of global fresh-water transports of importance to ocean circulation. Clim. Dyn. 4, 73–79.
Bruins, H.J., Keller, J., Klügel, A., Kisch, H.J., Katra, I., van der Plicht, J., 2019. Tephra in caves: distal deposits of the minoan Santorini eruption and the Campanian super-eruption. Quat. Int. 499, 135–147.
Buoncristiani, J.-F., Campy, M., 2004. Palaeogeography of the last two glacial episodes in the Massif Central, France. Dev. Quat. Sci. 2, 111–112.
Burjachs, F., López-García, J.M., Allué, E., Blain, H.A., Rivals, F., Bennàsar, M., Expósito, I., 2012. Palaeoecology of Neanderthals during Dansgaard–Oeschger cycles in northeastern Iberia (abric Romaní): from regional to global scale. Quat. Int. 247, 26–37.
Butzin, M., Köhler, P., Lohmann, G., 2017. Marine radiocarbon reservoir age simulations for the past 50,000 years. Geophys. Res. Lett. 44 (16), 8473–8480.
Cacho, I., Grimalt, J.O., Pelejero, C., Canals, M., Sierro, F.J., Flores, J.A., Shackleton, N., 1999. Dansgaard-oeschger and Heinrich event imprints in Alboran sea paleotemperatures. Paleoceanography 14 (6), 698–705.
Carraro, F., Sauro, U., 1979. Il Glacialismo "locale" Wurmiano del Massiccio del Grappa (Provincie di Treviso e di Vicenza). Geogr. Fis. Din. Quaternaria 2 (1), 6–16.
Cattani, L., 1990. Steppe environments at the margin of the Venetian pre-alps during the pleniglacial and late-glacial periods. In: In: Cremaschi, M. (Ed.), The Loess in Northern and Central Italy: a Loess Basin between the Alps and the Mediterranean Region, Quaderni di Geodinamica Alpina e Quaternaria, vol. 1. pp. 133–137.
Cattani, L., Renault-Miskovsky, J., 1983-84. Etude pollinique du remplissage de la Grotte du Broion (Vicenza, Italie). Paléoclimatologie du Würmien en Vénétie. Bullettin Association Française Étude du Quaternaire XVI (4), 197–212.
Cheng, H., Lawrence Edwards, R., Southon, J., Matsumoto, K., Feinberg, J.M., Sinha, A., Zhou, W., Li, H., Li, X., Xu, Y., Chen, S., Tan, M., Wang, Q., Wang, Y., Ning, Y., 2018. Atmospheric $^{14}C/^{12}C$ changes during the last glacial period from Hulu Cave. Science 362, 1293–1297.
Chiesa, S., Coltorti, M., Cremaschi, M., Ferraris, M., Prosperi, l., 1990. Loess sedimentation and quaternary deposits in the Marche province. In: In: Cremaschi, M. (Ed.), The Loess in Northern and Central Italy. A Loess Basin between the Alps and the Mediterranean Region, vol. 1. Quaderni di Geodinamica Alpina e Quaternaria, Milano, pp. 103–130.
Combourieu-Nebout, N., Turon, J.-L., Zahn, R., Capotondi, L., Londeix, L., Pahnke, K., 2002. Enhanced aridity and atmospheric high-pressure stability over the western Mediterranean during the North Atlantic cold events of the past 50 k. y. Geology 30, 863–866.
Combourieu-Nebout, N., Peyron, O., Dormoy, I., Desprat, S., Beaudouin, C., Kotthoff, U., Marret, F., 2009. Rapid climatic variability in the west Mediterranean during the last 25 000 years from high resolution pollen data. Clim. Past 5 (3), 503–521.
Copeland, L., Yazbeck, C., 2002. Inventory of stone age sites in Lebanon. In: New and Revised, Part III, vol. 55. Melanges de l'Universite Saint-Joseph, pp. 121–325.
Costa, A., Folch, A., Macedonio, G., Giaccio, B., Isaia, R., Smith, V.C., 2012. Quantifying volcanic ash dispersal and impact of the Campanian Ignimbrite super-eruption. Geophys. Res. Lett. 39 (10).
Cremaschi, M., 1990. The Loess in Northern and Central Italy. A Loess Basin between the Alps and the Mediterranean Region, vol. 1 Quaderni di Geodinamica Alpina e Quaternaria, Milano, Italy.
Cremaschi, M., 2004. Late Pleistocene loess. In: Antonioli, F., Vai, G.B. (Eds.), Litho-palaeoenvironmental Maps of Italy During the Last Two Climatic Extremes. Climex Maps Italy e Explanatory Notes, pp. 34–37 Bologna.
Cremaschi, M., Zerboni, A., Nicosia, C., Negrino, F., Rodnight, H., Spötl, C., 2015. Age, soil-forming processes, and archaeology of the loess deposits at the Apennine margin of the Po Plain (northern Italy). New insights from the Ghiardo area. Quat. Int. 376, 173–188.
Cremonesi, G., 1987. Due complessi d'arte del Paleolitico superiore: la Grotta Polesini e la Grotta delle Veneri. Atti del VI Convegno di Preistoria e Protostoria. Storia della Daunia 2, 35–50.
Crouvi, O., Amit, R., Enzel, Y., Gillespie, A.R., 2010. The role of active sand seas in the formation of desert loess. Quat. Sci. Rev. 29, 2087–2098.
Daniau, A.L., Sánchez-Goñi, M.F., Beaufort, L., Laggoun-Défarge, F., Loutre, M.F., Duprat, J., 2007. Dansgaard–Oeschger climatic variability revealed by fire emissions in southwestern Iberia. Quat. Sci. Rev. 26 (9–10), 1369–1383.
Daniau, A.L., Goñi, M.F.S., Duprat, J., 2009. Last glacial fire regime variability in western France inferred from microcharcoal preserved in core MD04-2845, Bay of Biscay. Quat. Res. 71 (3), 385–396.
Dansgaard, W., Johnsen, S.J., Clausen, H.B., Dahl-Jensen, D., Gundestrup, N.S., Hammer, C.U., Hvidberg, C.S., Steffensen, J.P., Sveinbjorndottir, A.E., Jouzel, J., Bond, G., 1993. Evidence for general instability of past climate from a 250-kyr ice-core record. Nature 364, 218–220.
Darfeuil, S., Ménot, G., Giraud, X., Rostek, F., Tachikawa, K., Garcia, M., Bard, É., 2016. Sea surface temperature reconstructions over the last 70 kyr off Portugal: biomarker data and regional modeling. Paleoceanography 31 (1), 40–65.
Darlas, A., Psathi, E., 2016. The middle and upper Paleolithic on the western coast of the Mani peninsula (southern Greece). In: Paleoanthropology of the Balkans and Anatolia. Springer, Dordrecht, pp. 95–117.
de Goër, H., 1972. La Planèze de Saint Flour: formes et dépots glaciaires. Annales de la faculté des Sciences de Clermont-Ferrand, vol. 48. pp. 1–204.
Delmas, M., 2015. The Last Maximum Ice Extent and subsequent deglaciation of the Pyrenees: an overview of recent research. Cuadernos de Investigación Geográfica 41, 359–387.
Delpiano, D., Peresani, M., Bertola, S., Cremaschi, M., Zerboni, A., 2019. Lashed by the wind: short-term middle Palaeolithic occupations within the loess-palaeosoil sequence at Monte Netto (northern Italy). Quat. Int. 502, 137–147.
Dini, M., Tozzi, C., 2012. La transizione paleolitico Medio-paleolitico superiore nella grotta La Fabbrica (Grosseto-Toscana). Atti della Società Toscana di Scienze Naturali - Memorie Serie A 117–119.
Douka, K., Higham, T., 2017. The chronological factor in understanding the middle and upper Paleolithic of Eurasia. Curr. Anthropol. 58 (S17), S480–S490.
Douka, K., Grimaldi, S., Boschian, G., del Lucchese, A., Higham, T.F., 2012. A new chronostratigraphic framework for the upper Palaeolithic of riparo Mochi (Italy). J. Hum. Evol. 62 (2), 286–299.
Douka, K., Bergman, C.A., Hedges, R.E.M., Wesselingh, F.P., Higham, T., 2013. Chronology of Ksar Akil (Lebanon) and implications for the colonization of Europe by anatomically modern humans. PLoS One 8, e72931.
Douka, K., Higham, T.F., Wood, R., Boscato, P., Gambassini, P., Karkanas, P., Peresani, M., Ronchitelli, A.M., 2014. On the chronology of the Uluzzian. J. Hum. Evol. 68, 1–13.
Drescher-Schneider, R., Jacquat, C., Schoch, W., 2007. Palaeobotanical investigations at the mammoth site of Niederweningen (Kanton Zürich). Switzerland. Quat. Int. 164–165, 113–129.
Ehlers, J., Gibbard, P.L., Hughes, P.D., 2011. Quaternary Glaciations e Extent and Chronology, vol. 15. Elsevier, Amsterdam, pp. 1126.
Engel, Z., Mentlík, P., Braucher, R., Minár, J., Léanni, L., Aster Team, 2015. Geomorphological evidence and ^{10}Be exposure ages for the last glacial maximum and deglaciation of the Velká and Malá Studená dolina valleys in the high Tatra mountains, central Europe. Quat. Sci. Rev. 124, 106–123.
European Environment Agency, 2015. European Ecosystem Assessment - Concept, Data, and Implementation. Contribution to Target 2 Action 5 Mapping and Assessment of Ecosystems and Their Services (MAES) of the EU Biodiversity Strategy to 2020. Technical Report 06/2015.
Falcucci, A., Peresani, M., 2018. Protoaurignacian core reduction procedures: blade and bladelet technologies at Fumane Cave. Lithic Technol. 43 (2), 125–140.
Falcucci, A., Conard, N.J., Peresani, M., 2017. A critical assessment of the Protoaurignacian lithic technology at Fumane Cave and its implications for the definition of the earliest Aurignacian. PLoS One 12 (12), e0189241.
Farquhar, G.D., 1997. Carbon dioxide and vegetation. Science 278 (5342), 1411.
Fedele, F.G., Giaccio, B., Isaia, R., Orsi, G., 2003. The Campanian ignimbrite eruption, Heinrich event 4. In: Robock, A., Oppenheimer, C. (Eds.), the Paleolithic Change in Europe: a High-Resolution Investigation. Volcanism and Earth's Atmosphere. AGU Geophys, Washington, DC), pp. 301–325.
Fedele, F.G., Giaccio, B., Hajdas, I., 2008. Timescales and cultural process at 40,000 BP in the light of the Campanian Ignimbrite eruption, western Eurasia. J. Hum. Evol. 55, 834–857.
Federici, P., Ribolini, A., Spagnolo, M., 2017. Glacial history of the Maritime Alps from the last glacial maximum to the little ice age. Geological Society, London, Special Publications 433 (1), 137–159.
Ferraro, F., 2009. Age, sedimentation, and soil formation in the Val Sorda loess sequence, Northern Italy. Quat. Int. 204, 54–64.
Fischer, H., Fundel, F., Ruth, U., Twarloh, B., Wegner, A., Udisti, R., Becagli, S., Castellano, E., Morganti, A., Severi, M., Wolff, E., Littot, G., Röthlisberger, R.,

Mulvaney, R., Hutterli, M.A., Kaufmann, P., Federer, U., Lambert, F., Bigler, M., Hansson, M., Jonsell, U., de Angelis, M., Boutron, C., Siggaard-Andersen, M.-L., Steffensen, J.P., Barbante, C., Gaspari, V., Gabrielli, P., Wagenbach, D., 2007a. Reconstruction of millennial changes in dust emission, transport and regional sea ice coverage using the deep EPICA ice cores from the Atlantic and Indian Ocean sector of Antarctica. Earth Planet. Sci. Lett. 260 (1), 340–354.

Fischer, H., Siggaard-Andersen, M.L., Ruth, U., Röthlisberger, R., Wolff, E., 2007b. Glacial/interglacial changes in mineral dust and sea-salt records in polar ice cores: sources, transport, and deposition. Rev. Geophys. 45 (1).

Fleitmann, D., Cheng, H., Badertscher, S., Edwards, R.L., Mudelsee, M., Göktürk, O.M., Fankhauser, A., Pickering, R., Raible, C.C., Matter, A., Kramers, J., Tüysüz, O., 2009. Timing and climatic impact of Greenland interstadials recorded in stalagmites from northern Turkey. Geophys. Res. Lett. 36 (19).

Fletcher, W.J., Sánchez Goñi, M.F., 2008. Orbital-and sub-orbital-scale climate impacts on vegetation of the western Mediterranean basin over the last 48,000 yr. Quat. Res. 70 (3), 451–464.

Fletcher, W.J., Sánchez Goñi, M.F., Peyron, O., Dormoy, I., 2010a. Abrupt climate changes of the last deglaciation detected in a Western Mediterranean forest record. Clim. Past 6, 245–264.

Fletcher, W.J., Sánchez Goñi, M.F., Allen, J.R.M., Cheddadi, R., Comborieu-Nebout, N., Huntley, B., Lawson, I., Londeix, L., Magri, D., Margari, V., Müller, U.C., Naughton, F., Novenko, E., Roucoux, K., Tzedakis, P.C., 2010b. Millennial scale variability during the last glacial in vegetation records from Europe. Quat. Sci. Rev. 29 (21–22), 2839–2864.

Floss, H., 2003. Did they meet or not? Observations on Châtelperronian and Aurignacian settlement patterns in eastern France. In: In: Zilhao & Errico (Ed.), The chronology of the Aurignacian and of the transitional technocomplexes. Dating, stratigraphies, cultural implications. Actes 14e Congrès UISPP, Université de Liège, Belgique, 2-8 sept. 2001, vol. 33. Trabalhos de Arqueologia n°, pp. 273–287.

Flückiger, J., Knutti, R., White, J.W., 2006. Oceanic processes as potential trigger and amplifying mechanisms for Heinrich events. Paleoceanography 21 (2).

Follieri, M., Magri, D., Sadori, L., 1988. 250,000-year pollen record from Valle di Castiglione (Roma). Pollen Spores 30, 329–356.

Follieri, M., Giardini, M., Magri, D., Sadori, L., 1998. Palynostratigraphy of the last glacial period in the volcanic region of central Italy. Quat. Int. 47, 3–20.

Fontana, A., Mozzi, P., Marchetti, M., 2014. Alluvial fans and megafans along the southern side of the Alps. Sediment. Geol. 301, 150–171.

Forno, M.G., Gianotti, F., Racca, G., 2010. Significato paleoclimatico dei rapporti tra il glacialismo principale e quello tributario nella Bassa Valle della Dora Baltea. Il Quat. 23, 105–124.

Franciscus, R.G., 1999. Neandertal nasal structures and upper respiratory tract "specialization". Proc. Natl. Acad. Sci. 96 (4), 1805–1809.

Frechen, M., Horváth, E., Gábris, G., 1997. Geochronology of middle and upper Pleistocene loess sections in Hungary. Quat. Res. 48, 291–312.

Furlanetto, G., Ravazzi, C., Badino, F., Brunetti, M., Champvillair, E., Maggi, V., 2019. Elevational transects of modern pollen samples: site-specific temperatures as a tool for palaeoclimate reconstructions in the Alps. Holocene 29 (2), 271–286.

Gambassini, P., 1997. Il Paleolitico di Castelcivita: culture e ambiente. Electa, Napoli, Italy.

Genty, D., Blamart, D., Ouahdi, R., Gilmour, M., Baker, A., Jouzel, J., Van-Exter, S., 2003. Precise dating of Dansgaard–Oeschger climate oscillations in western Europe from stalagmite data. Nature 421 (6925), 833.

Genty, D., Blamart, D., Ghaleb, B., Plagnes, V., Causse, C., Bakalowicz, M., Zouari, K., Chkir, N., Hellstrom, J., Wainer, K., Bourges, F., 2006. Timing and dynamics of the last deglaciation from European and North African $\delta^{13}C$ stalagmite profiles—comparison with Chinese and South Hemisphere stalagmites. Quat. Sci. Rev. 25 (17–18), 2118–2142.

Genty, D., Combourieu-Nebout, N., Peyron, O., Blamart, D., Wainer, K., Mansuri, F., Ghaleb, B., Isabello, L., Dormoy, I., von Grafenstein, U., Bonelli, S., Landais, A., Brauer, A., 2010. Isotopic characterization of rapid climatic events during OIS3 and OIS4 in Villars Cave stalagmites (SW-France) and correlation with Atlantic and Mediterranean pollen records. Quat. Sci. Rev. 29 (19), 2799–2820.

Giaccio, B., Hajdas, I., Peresani, M., Fedele, F.G., Isaia, R., 2006. In: Conard, N.J. (Ed.), The Campanian Ignimbrite Tephra and its Relevance for the Timing of the Middle to Upper Palaeolithic Shift. When Neanderthals and Modern Humans Met. Kerns Verlag, Tübingen, Germany), pp. 343–375.

Giaccio, B., Isaia, R., Fedele, F.G., Di Canzio, E., Hoffecker, J., Ronchitelli, A., Sinitsyn, A.A., Anikovich, M., Lisitsyn, S.N., Popov, V.V., 2008. The Campanian ignimbrite and Codola tephra layers: two temporal/stratigraphic markers for the early upper Palaeolithic in southern Italy and eastern Europe. J. Volcanol. Geotherm. Res. 177, 208–226.

Giaccio, B., Hajdas, I., Isaia, R., Deino, A., Nomade, S., 2017. High-precision ^{14}C and $^{40}Ar/^{39}Ar$ dating of the Campanian Ignimbrite (Y-5) reconciles the time-scales of climatic-cultural processes at 40 ka. Sci. Rep. 7, 45940.

Gianotti, F., Forno, M.G., Ivy-Ochs, S., Monegato, G., Pini, R., Ravazzi, C., 2015. Stratigraphy of the Ivrea morainic amphitheatre (NW Italy): an updated synthesis. Alpine Mediterr. Quat. 28, 29–58.

Giraudi, C., Giaccio, B., 2016. Middle Pleistocene glaciations in the Apennines, Italy: new chronological data and preservation of the glacial record. In: In: Hughes, P.D., Woodward, J.C. (Eds.), Quaternary Glaciation in the Mediterranean Mountains, vol. 433. Geological Society, London, Special Publications, pp. 161–178.

Govin, A., Capron, E., Tzedakis, P.C., Verheyden, S., Ghaleb, B., Hillaire-Marcel, C., St-Onge, G., Stoner, J.S., Bassinot, F., Bazin, L., Blunier, T., Combourieu-Nebout, N., El Ouahabi, A., Genty, D., Gersonde, R., Jimenez-Amat, P., Landais, A., Martrat, B., Masson-Delmotte, V., Parrenin, F., Seidenkrantz, M.-S., Veres, D., Waelbroeck, C., Zahn, R., 2015. Sequence of events from the onset to the demise of the Last Interglacial: evaluating strengths and limitations of chronologies used in climatic archives. Quat. Sci. Rev. 129, 1–36.

Grant, K.M., Rohling, E.J., Bar-Matthews, M., Ayalon, A., Medina-Elizalde, M., Ramsey, C.B., Satow, C., Roberts, A.P., 2012. Rapid coupling between ice volume and polar temperature over the past 150,000 years. Nature 491 (7426), 744.

Greenbaum, G., Friesem, D.E., Hovers, E., Feldman, M.W., Kolodny, O., 2019. Was inter-population connectivity of Neanderthals and modern humans the driver of the Upper Paleolithic transition rather than its product? Quat. Sci. Rev. 217, 316–329.

Gromig, R., Mechernich, S., Ribolini, A., Wagner, B., Zanchetta, G., Isola, I., Bini, M., Dunai, T., 2018. Evidence for a younger Dryas deglaciation in the Galicica mountains (FYROM) from cosmogenic ^{36}Cl. Quat. Int. 464, 352–363.

Guillevic, M., Bazin, L., Landais, A., Stowasser, C., Masson-Delmotte, V., Blunier, T., Eynaud, F., Falourd, S., Michel, E., Minster, B., Popp, T., Prié, F., Vinther, B.M., 2014. Evidence for a three-phase sequence during Heinrich Stadial 4 using a multiproxy approach based on Greenland ice core records. Clim. Past 10 (6), 2115–2133.

Guiot, J., Reille, M., de Beaulieu, J.L., Pons, A., 1992. Calibration of the climatic signal in a new pollen sequence from La Grande Pile. Clim. Dyn. 6 (3–4), 259–264.

Güleç, E., Kuhn, S.L., Stiner, M.C., 2002. The early upper Palaeolithic of Üçağızlı cave, Turkey. Antiquity 76 (293), 615–616.

Haase, D., Fink, J., Haase, G., Ruske, R., Pécsi, M., Richter, H., Altermann, M., Jäger, K.D., 2007. Loess in Europe - its spatial distribution based on a European loess map, scale 1: 2,500,000. Quat. Sci. Rev. 26 (9–10), 1301–1312.

Haesaerts, P., Borziac, I., Chekha, V.P., Chirica, V., Damblon, F., Drozdov, N.I., Orlova, L.A., Pirson, S., van der Plicht, J., 2009. Climatic signature and radiocarbon chronology of middle and late pleniglacial loess from Eurasia: comparison with the marine and Greenland records. Radiocarbon 51 (1), 301–318.

Harrison, S.P., Sánchez Goñi, M.F., 2010. Global patterns of vegetation response to millennial-scale variability and rapid climate change during the last glacial period. Quat. Sci. Rev. 29 (21–22), 2957–2980.

Heinrich, H., 1988. Origin and consequences of cyclic ice rafting in the northeast Atlantic Ocean during the past 130,000 years. Quat. Res. 29 (2), 142–152.

Hemming, S.R., 2004. Heinrich events: massive late Pleistocene detritus layers of the North Atlantic and their global climate imprint. Rev. Geophys. 42 (1), RG1005. https://doi.org/10.1029/2003RG000128.

Hershkovitz, I., Marder, O., Ayalon, A., Bar-Matthews, M., Yasur, G., Boaretto, E., Caracuta, V., Alex, B., Frumkin, A., Goder-Goldberger, M., Gunz, P., Holloway, R.L., Latimer, B., Lavi, R., Matthews, A., Slon, Vi, Bar-Yosef Mayer, D., Berna, F., Bar-Oz, G., Yeshurun, R., May, H., Hans, M.G., Weber, G.W., Barzilai, O., 2015. Levantine cranium from Manot Cave (Israel) foreshadows the first European modern humans. Nature 520 (7546), 216.

Higham, T., 2011. European Middle and Upper Palaeolithic radiocarbon dates are often older than they look: problems with previous dates and some remedies. Antiquity 85 (327), 235–249.

Higham, T., Brock, F., Peresani, M., Broglio, A., Wood, R., Douka, K., 2009. Problems with radiocarbon dating the middle to upper Palaeolithic transition in Italy. Quat. Sci. Rev. 28 (13–14), 1257–1267.

Higham, T., Douka, K., Wood, R., Ramsey, C.B., Brock, F., Basell, L., Camps, M., Arrizabalaga, A., Baena, J., Barroso-Ruiz, C., Bergman, C., Boitard, C., Boscato, P., Caparros, M., Conard, N.J., Draily, C., Froment, A., Galvan, B., Gambassini, P., Garcia-Moreno, A., Grimaldi, S., Haesaerts, P., Holt, B., Iriarte-Chiapusso, M.J., Jelinek, A., Jorda Pardo, J.F., Maillo-Fernandez, J.M., Marom, A., Maroto, J., Menendez, M., Metz, L., Morin, E., Moroni, A., Negrino, F., Panagopoulou, E., Peresani, M., Pirson, S., de la Rasilla, M., Riel-Salvatore, J., Ronchitelli, A., Santamaria, D., Semal, P., Slimak, L., Soler, J., Soler, N., Villaluenga, A., Pinhasi, R., Jacobi, R., 2014. The timing and spatiotemporal patterning of Neanderthal disappearance. Nature 512, 306–309.

Hoffecker, J.F., 2009. The spread of modern humans in Europe. Proc. Natl. Acad. Sci. 106 (38), 16040–16045.

Hoffecker, J.F., Holliday, V.T., Anikovich, M.V., Sinitsyn, A.A., Popov, V.V., Lisitsyn, S.N., Levkovskaya, G.M., Pospelova, G.A., Forman, S.L., Giaccio, B., 2008. From the bay of Naples to the river Don: the Campanian ignimbrite eruption and the middle to upper Paleolithic transition in eastern Europe. J. Hum. Evol. 55, 858–870.

Holtmeier, F.K., 1985. Climatic stress influencing the physiognomy of trees at the polar and mountain timberline. Eidgenössische Anstalt für das Forstliche Versuchswesen, Berichte 270, 31–40.

Holtmeier, F.K., 2009. Mountain Timberlines: Ecology, Patchiness, and Dynamics, vol. 36 Springer Science & Business Media.

Hublin, J.-J., 2014. The modern human colonization of western Eurasia: when and where? Quat. Sci. Rev. 1–17.

Hublin, J.-J., 2015. The modern human colonization of western Eurasia: when and where? Quat. Sci. Rev. 18, 194–210.

Hughes, P.D., Woodward, J.C., 2016. Quaternary glaciation in the Mediterranean mountains: a new synthesis. In: In: Hughes, P.D., Woodward, J.C. (Eds.), Quaternary Glaciation in the Mediterranean Mountains, vol. 433. Geological Society, London, pp. 1–23. https://doi.org/10.1144/SP433.14. Special Publications.

Hughes, A.L.C., Gyllencreutz, R., Lohne, Ø.S., Mangerud, J., Svendsen, J.I., 2016. The last Eurasian ice sheets - a chronological database and time-slice reconstruction, DATED-1. Boreas 45, 1–45.

Hussain, S.T., Floss, H., 2016. Streams as entanglement of nature and culture: European Upper Paleolithic river systems and their role as features of spatial organization. J. Archaeol. Method Theory 23 (4), 1162–1218.

Iglesias, V., Yospin, G.I., Whitlock, C., 2015. Reconstruction of fire regimes through integrated paleoecological proxy data and ecological modeling. Front. Plant Sci. 5, 785.

Ivy-Ochs, S., Kerschner, H., Reuther, A., Preusser, F., Heine, K., Maisch, M., Kubik, P.W., Schlüchter, C., 2008. Chronology of the last glacial cycle in the European Alps. J. Quat. Sci. 23, 559–573.

Ivy-Ochs, S., Lucchesi, S., Baggio, P., Fioraso, G., Gianotti, G., Monegato, G., Graf, A.A., Akscar, N., Christl, M., Carraro, F., Forno, M.G., Schlüchter, C., 2018. New geomorphological and chronological constraints for glacial deposits in the Rivoli-Avigliana end-moraine system and the lower Susa Valley (Western Alps, NW Italy). J. Quat. Sci. 33, 550–562.
Jobbagy, E.G., Jackson, R.B., 2000. Global controls of forest line elevation in the northern and southern hemispheres. Glob. Ecol. Biogeogr. 9 (3), 253–268.
Jorda, M., Rosique, T., Evin, J., 2000. Données nouvelles sur l'age du dernier maximum glaciaire dans les Alpes méridionales françaises. Comptes Rendus Acad. Sci. - Ser. IIA Earth Planet. Sci. 331, 187–193.
Kelly, M.A., Kubik, P.W., Von Blanckenburg, F., Schlüchter, C., 2004. Surface exposure dating of the Great Aletsch Glacier Egesen moraine system, western Swiss Alps, using the cosmogenic nuclide 10Be. J. Quat. Sci. 19 (5), 431–441.
Kindler, P., Guillevic, M., Baumgartner, M., Schwander, J., Landais, A., Leuenberger, M., 2014. Temperature reconstruction from 10 to 120 kyr b2k from the NGRIP ice core. Clim. Past 10 (2), 887–902.
Körner, C., Paulsen, J., 2004. A world-wide study of high-altitude treeline temperatures. J. Biogeogr. 31 (5), 713–732.
Kuhlemann, J., Rohling, E.J., Krumrei, I., Kubik, P., Ivy-Ochs, S., Kucera, M., 2008. Regional synthesis of Mediterranean atmospheric circulation during the last glacial maximum. Science 321 (5894), 1338–1340.
Kuhlemann, J., Milivojevic, M., Krumrei, I., Kubik, P.W., 2009. Last glaciation of the Sara range (Balkan peninsula): increasing dryness from the LGM to the Holocene. Austrian J. Earth Sci. 102, 146–158.
Kuhn, S.L., Stiner, M.C., Güleç, E., Özer, I., Yilmaz, H., Baykara, I., Açikkol, A., Goldberg, P., Molina, K.M., Ünay, E., Suata-Alpaslan, F., 2009. The early upper Paleolithic occupations at Üçağızlı cave (Hatay, Turkey). J. Hum. Evol. 56 (2), 87–113.
Kukla, G.J., 1975. Loess stratigraphy of central Europe. In: Butzer, K.W., Isaac, L.I. (Eds.), After the Australopithecines. Mouton Publishers, The Hague, pp. 99–187.
Lambeck, K., Purcell, A., Zhao, J., Svensson, N.-O., 2010. The Scandinavian ice sheet: from MIS 4 to the end of the last glacial maximum. Boreas 39, 410–435.
Lambeck, K., Rouby, H., Purcell, A., Sun, Y., Sambridge, M., 2014. sea level and global ice volumes from the last glacial maximum to the Holocene. Proc. Natl. Acad. Sci. 111 (43), 15296–15303.
Lehmkuhl, F., Bösken, J., Hošek, J., Sprafke, T., Marković, S.B., Obreht, I., Hambach, U., Sümegi, P., Thiemann, A., Steffens, S., Lindner, H., Veres, D., Zeeden, C., 2018a. Loess distribution and related quaternary sediments in the Carpathian basin. J. Maps 14, 673–682.
Lehmkuhl, F., Pötter, S., Pauligk, A., Bösken, J., 2018b. Loess and other Quaternary sediments in Germany. J. Maps 14, 330–340.
Leonardi, P., Broglio, A., 1966. Datazione assoluta di un'industria musteriana della grotta del Broion. Rivista di Scienze Preistoriche 21 (2), 397–405.
Leroy, S.A.G., Giralt, S., Francus, P., Seret, G., 1996. The high sensitivity of the palynological record in the Vico maar lacustrine sequence (Latium, Italy) highlights the climatic gradient through Europe for the last 90 ka. Quat. Sci. Rev. 15 (2–3), 189–201.
Lézine, A.M., Von Grafenstein, U., Andersen, N., Belmecheri, S., Bordon, A., Caron, B., Cazet, J.-P., Erlenkeuser, H., Fouache, E., Grenier, C., Huntsman-Mapila, P., Hureau-Mazaudier, D., Manelli, D., Mazaud, A., Robert, C., Sulpizio, R., Tiercelin, J.-J., Zanchetta, G., Zeqollari, Z., 2010. Lake Ohrid, Albania, provides an exceptional multi-proxy record of environmental changes during the last glacial–interglacial cycle. Palaeogeogr. Palaeoclimatol. Palaeoecol. 287 (1–4), 116–127.
Lindner, H., Lehmkuhl, F., Zeeden, C., 2017. Spatial loess distribution in the eastern Carpathian Basin: a novel approach based on geoscientific maps and data. J. Maps 13, 173–181.
Lisiecki, L.E., Raymo, M.E., 2005. A Pliocene-Pleistocene stack of 57 globally distributed benthic $\delta^{18}O$ records. Paleoceanography 20 (1).
Lowe, J., Barton, N., Blockley, S., Ramsey, C.B., Cullen, V.L., Davies, W., Gamble, C., Grant, K., Hardiman, M., Housley, R., Lane, C.S., Lee, S., Lewis, M., MacLeod, A., Menzies, M., Müller, W., Pollard, M., Price, C., Roberts, A.P., Rohling, E.J., Satow, C., Smith, V.C., Stringer, C.B., Tomlinson, E.L., White, D., Albert, P., Arienzo, I., Barker, G., Borić, D., Carandente, A., Civetta, L., Ferrier, C., Guadelli, J.-L., Karkanas, P., Koumouzelis, M., Müller, U.C., Orsi, G., Pross, J., Rosi, M., Shalamanov-Korobar, L., Sirakov, N., Tzedakis, P.C., 2012. Volcanic ash layers illuminate the resilience of Neanderthals and early modern humans to natural hazards. Proc. Natl. Acad. Sci. 109, 13532–13537.
Magri, D., 1994. Late-Quaternary changes of plant biomass as recorded by pollen-stratigraphical data: a discussion of the problem at Valle di Castiglione, Italy. Rev. Palaeobot. Palynol. 81 (2–4), 313–325.
Magri, D., 1999. Late quaternary vegetation history at Lagaccione near Lago di Bolsena (central Italy). Rev. Palaeobot. Palynol. 106 (3–4), 171–208.
Magri, D., 2008. Two long micro-charcoal records from central Italy. In: Proceedings of the Third International Meeting of Anthracology, BAR International Series 1807. pp. 167–175.
Magri, D., Sadori, L., 1999. Late Pleistocene and Holocene pollen stratigraphy at Lago di Vico, central Italy. Veg. Hist. Archaeobotany 8 (4), 247–260.
Makos, M., Rinterknecht, V., Braucher, R., Toloczko-Pasek, A., ASTER Team, 2018. Last glacial maximum and Lateglacial in the polish high Tatra mountains - revised deglaciation chronology based on the ^{10}Be exposure age dating. Quat. Sci. Rev. 187, 130–156.
Mangerud, J., Gulliksen, S., Larsen, E., 2010. ^{14}C-dated fluctuations of the western flank of the Scandinavian Ice Sheet 45–25 kyr BP compared with Bølling–Younger Dryas fluctuations and Dansgaard–Oeschger events in Greenland. Boreas 39 (2), 328–342.
Marciani, G, Ronchitelli, A., Arrighi, S., Badino, F., Bortolini, E., P., Boscato, Boschin, F., Crezzini, J., Delpiano, D., Falcucci, A., Figus, C., Lugli, F., Negrino, F., Oxilia G., Romandini, M., Riel-Salvatore, J., Spinapolice, E. E., Peresani, M., Moroni, A., Benazzi, S., this issue. Lithic Techno-Complexes in Italy from 50 to 39 Thousand Years BP: an Overview of Cultural and Technological Changes across the Middle-Upper Palaeolithic Boundary.
Marcott, S.A., Clark, P.U., Padman, L., Klinkhammer, G.P., Springer, S.R., Liu, Z., Otto-Bliesner, B.L., Carlson, A.E., Ungerer, A., Padman, J., He, F., Cheng, J., Schmittner, A., 2011. Ice-shelf collapse from subsurface warming as a trigger for Heinrich events. Proc. Natl. Acad. Sci. 108 (33), 13415–13419.
Margari, V., Gibbard, P.L., Bryant, C.L., Tzedakis, P.C., 2009. Character of vegetational and environmental changes in southern Europe during the last glacial period; evidence from Lesvos Island, Greece. Quat. Sci. Rev. 28 (13–14), 1317–1339.
Margherita, C., Oxilia, G., Barbi, V., Panetta, D., Hublin, J.-J., Lordkipanidze, D., Meshveliani, T., Jakeli, N., Matskevich, Z., Bar-Yosef, O., Belfer-Cohen, A., Pinhasi, R., Benazzi, S., 2017. Morphological description and morphometric analyses of the Upper Palaeolithic human remains from Dzudzuana and Satsurblia caves, western Georgia. J. Hum. Evol. 113, 83–90.
Mariani, G.S., Cremaschi, M., Zerboni, A., Zuccoli, L., Trombino, L., 2018. Geomorphological map of the Mt. Cusna ridge (northern Apennines, Italy): evolution of a Holocene landscape. J. Maps 14, 392–401.
Marković, S.B., Stevens, T., Kukla, G.J., Hambach, U., Fitzsimmons, K.E., Gibbard, P., Buggle, B., Zech, M., Guo, Z., Hao, Q., Wu, H., O'Hara Dhand, K., Smalley, I.J., Újvári, G., Sümegi, P., Timar-Gabor, A., Veres, D., Sirocko, F., Vasiljević, D.A., Jary, Z., Svensson, A., Jović, V., Lehmkuhl, F., Kovács, J., Svirčev, Z., 2015. Danube loess stratigraphy -Towards a pan-European loess stratigraphic model. Earth Sci. Rev. 148, 228–258.
Marti, A., Folch, A., Costa, A., Engwell, S., 2016. Reconstructing the plinian and co-ignimbrite sources of large volcanic eruptions: a novel approach for the Campanian Ignimbrite. Sci. Rep. 6, 21220.
Martrat, B., Grimalt, J.O., Shackleton, N.J., de Abreu, L., Hutterli, M.A., Stocker, T.F., 2007. Four climate cycles of recurring deep and surface water destabilizations on the Iberian margin. Science 317 (5837), 502–507.
Maselli, V., Trincardi, F., Asioli, A., Ceregato, A., Rizzetto, F., Taviani, M., 2014. Delta growth and river valleys: the influence of climate and sea level changes on the South Adriatic shelf (Mediterranean Sea). Quat. Sci. Rev. 99, 146–163.
McDermott, F., 2004. Palaeo-climate reconstruction from stable isotope variations in speleothems: a review. Quat. Sci. Rev. 23 (7–8), 901–918.
McManus, J.F., Oppo, D.W., Cullen, J.L., 1999. A 0.5-million-year record of millennial scale climate variability in the North Atlantic. Science 283 (5404), 971–975.
Mellars, P., 2006. Archeology and the dispersal of modern humans in Europe: deconstructing the "Aurignacian". Evol. Anthropol.: Issues, News, and Reviews: Issues, News, and Reviews 15 (5), 167–182.
Mihailović, D., Whallon, R., 2017. Crvena Stijena revisited: the late Mousterian assemblages. Quat. Int. 450, 36–49.
Miko, S., Ilijanić, N., Hasan, O., Razum, I., Durn, T., Brunović, D., Papatheodorou, G., Bakrač, K., Hajek, Tadesse, V., Šparica Miko, M., Crmarić, R., 2017. Submerged karst landscapes of the eastern Adriatic. In: 5th Regional Scientific Meeting on Quaternary Geology Dedicated to Geohazards and Final Conference of the LoLADRIA Project "Submerged Pleistocene Landscapes of the Adriatic Sea".
Moine, O., Antoine, P., Hatté, C., Landais, A., Mathieu, J., Prud'homme, C., Rousseau, D.-D., 2017. The impact of Last Glacial climate variability in west-European loess revealed by radiocarbon dating of fossil earthworm granules. Proc. Natl. Acad. Sci. 114 (24), 6209–6214.
Monegato, G., 2012. Local glaciers in the Julian Prealps (NE Italy) during the last glacial maximum. Alpine Mediterr. Quat. 25, 5–14.
Monegato, G., Ravazzi, C., Donegana, M., Pini, R., Calderoni, G., Wick, L., 2007. Evidence of a two-fold glacial advance during the last glacial maximum in the Tagliamento end moraine system (eastern Alps). Quat. Res. 68, 284–302.
Monegato, G., Scardia, G., Hajdas, I., Rizzini, F., Piccin, A., 2017. The Alpine LGM in the boreal ice-sheets game. Sci. Rep. 7, 2078.
Moreno, A., Stoll, H., Jiménez-Sánchez, M., Cacho, I., Valero-Garcés, B., Ito, E., Edwards, R.L., 2010. A speleothem record of glacial (25–11.6 kyr BP) rapid climatic changes from northern Iberian Peninsula. Glob. Planet. Chang. 71 (3–4), 218–231.
Morley, M.W., Woodward, J.C., 2011. The Campanian ignimbrite at Crvena Stijena rockshelter in Montenegro. Quat. Res. 75, 683–696.
Moroni, A., Boscato, P., Ronchitelli, A., 2013. What roots for the Uluzzian? Modern behaviour in Central-Southern Italy and hypotheses on AMH dispersal routes. Quat. Int. 316, 27–44.
Moroni, A., Ronchitelli, A., Arrighi, S., Aureli, D., Bailey, Boscato, P., Boschin, F., Capecchi, G., Crezzini, J., Douka, K., Marciani, G., Panetta, D., Ranaldo, F., Ricci, S., Scaramucci, S., Spagnolo, V., Benazzi, S., Gambassini, P., 2018. Grotta del Cavallo (Apulia–Southern Italy). The Uluzzian in the mirror. J. Anthropol. Sci. 96, 1–36.
Moseley, G.E., Spötl, C., Svensson, A., Cheng, H., Brandstätter, S., Edwards, R.L., 2014. Multi-speleothem record reveals tightly coupled climate between central Europe and Greenland during Marine Isotope Stage 3. Geology 42 (12), 1043–1046.
Müller, U.C., Pross, J., Bibus, E., 2003. Vegetation response to rapid climate change in Central Europe during the past 140,000 yr based on evidence from the Füramoos pollen record. Quat. Res. 59 (2), 235–245.
Müller, U.C., Pross, J., Tzedakis, P.C., Gamble, C., Kotthoff, U., Schmiedl, G., Wulf, S., Christanis, K., 2011. The role of climate in the spread of modern humans into Europe. Quat. Sci. Rev. 30 (3–4), 273–279.
Naughton, F., Sánchez Goñi, M.F., Kageyama, M., Bard, E., Duprat, J., Cortijo, E., Desprat, S., Malaizé, B., Joly, C., Rostek, F., Turon, J.-L., 2009. Wet to dry climatic trend in north-western Iberia within Heinrich events. Earth Planet. Sci. Lett. 284, 329–342.
NGRIP members, 2004. High-resolution record of Northern Hemisphere climate extending into the last interglacial period. Nature 431, 147–151.
Nigst, P.R., Haesaerts, P., Damblon, F., Frank-Fellner, C., Mallol, C., Viola, B., Götzingerh, M., Nivena, L., Trnkai, G., Hublin, J.J., 2014. Early modern human settlement of

Europe north of the Alps occurred 43,500 years ago in a cold steppe-type environment. Proc. Natl. Acad. Sci. 111 (40), 14394–14399.
Obruchev, V.A., 1914. The problem of North African loess. Zemlevedenie 4, 26–31 (in Russian).
Oliva, M., Palacios, D., Fernández-Fernández, J.M., Rodríguez-Rodríguez, L., García-Ruiz, J.M., Andrés, N., Carrasco, R.M., Pedraza, J., Pérez-Alberti, A., Valcárcel, M., Hughes, P.D., 2019. Late quaternary glacial phases in the Iberian peninsula. Earth Sci. Rev. 192, 564–600.
Pailler, D., Bard, E., 2002. High frequency palaeoceanographic changes during the past 140000 yr recorded by the organic matter in sediments of the Iberian Margin. Palaeogeogr. Palaeoclimatol. Palaeoecol. 181 (4), 431–452.
Pallàs, R., Rodés, A., Braucher, R., Bourlès, D., Delmas, M., Calvet, M., Gunnell, Y., 2010. Small isolated glacial catchments as priority targets for cosmogenic surface exposure dating of Pleistocene climate fluctuations, southeastern Pyrenees. Geology 38, 891–894.
Palma di Cesnola, A., 1989. L'Uluzzien: faciès italien du Leptolithique archaïque. L'Anthropologie 93 (4), 783–812.
Panagiotopoulos, K., Böhm, A., Leng, M.J., Wagner, B., Schäbitz, F., 2014. Climate variability over the last 92 ka in SW Balkans from analysis of sediments from Lake Prespa. Clim. Past 10 (2), 643–660.
Pellegrini, C., Maselli, V., Gamberi, F., Asioli, A., Bohacs, K.M., Drexler, T.M., Trincardi, F., 2017. How to make a 350-m-thick lowstand systems tract in 17,000 years: The Late Pleistocene Po River (Italy) lowstand wedge. Geology 45 (4), 327–330.
Pellegrini, C., Asioli, A., Bohacs, K.M., Drexler, T., Feldman, H.R, Sweet, M.L, Maselli, V., Rovere, M., Gamberia, F., Dalla Valle, G., Trincardi, F., 2018. The late Pleistocene Po River lowstand wedge in the Adriatic Sea: Controls on architecture variability and sediment partitioning. Mar. Pet. Geol. 96, 16–50.
Peresani, M., 2011. The end of the Middle Palaeolithic in the Italian Alps. An overview on Neandertal land-use, subsistence and technology. In: Conards, N., Richter, J. (Eds.), Neanderthal Lifeways, Subsistence and Technology. One Hundred Fifty Years of Neanderthal Study. Vertebrate Paleobiology and Paleoanthropology Series, Springer ed. pp. 249–259.
Peresani, M., 2014. L'Uluzzien en Italie. In: Otte, M. (Ed.), Néandertal/Cro-Magnon. La Rencontre. Editions Errance, Arles, pp. 61–80.
Peresani, M., Cremaschi, M., Ferraro, F., Falgueres, C., Bahain, J.J., Gruppioni, G., Sibilia, E., Quarta, G., Calcagnile, L., Dolo, J.M., 2008. Age of the final middle Palaeolithic and Uluzzian levels at Fumane cave, northern Italy, using 14C, ESR, 234U/230Th and thermoluminescence methods. J. Archaeol. Sci. 35 (11), 2986–2996.
Peresani, M., Cristiani, E., Romandini, M., 2016. The Uluzzian technology of grotta di Fumane and its implication for reconstructing cultural dynamics in the middle–upper Palaeolithic transition of western Eurasia. J. Hum. Evol. 91, 36–56.
Peresani, M., Bertola, S., Delpiano, D., Benazzi, S., Romandini, M., 2018. The Uluzzian in the north of Italy: insights around the new evidence at Riparo Broion. Archaeol. Anthropol. Sci. 1–34.
Peresani, M., Bertola, S., Delpiano, D., Benazzi, S., Romandini, M., 2019. The Uluzzian in the north of Italy: insights around the new evidence at Riparo Broion. Archaeol. Anthropol. Sci. 11, 3503–3536.
Peters, C., Walden, J., Austin, W.E., 2008. Magnetic signature of European margin sediments: Provenance of ice-rafted debris and the climatic response of the British ice sheet during Marine Isotope Stages 2 and 3. J. Geophys. Res.: Earth Surf. 113 (F3).
Petersen, S.V., Schrag, D.P., Clark, P.U., 2013. A new mechanism for Dansgaard-Oeschger cycles. Paleoceanography 28 (1), 24–30.
Peterson, L.C., Haug, G.H., 2006. Variability in the mean latitude of the Atlantic intertropical convergence zone as recorded by riverine input of sediments to the Cariaco basin (Venezuela). Palaeogeogr. Palaeoclimatol. Palaeoecol. 234 (1), 97–113.
Pini, R., Ravazzi, C., Donegana, M., 2009. Pollen stratigraphy, vegetation and climate history of the last 215 ka in the Azzano Decimo core (plain of Friuli, north-eastern Italy). Quat. Sci. Rev. 28, 1268–1290.
Pini, R., Ravazzi, C., Reimer, P.J., 2010. The vegetation and climate history of the last glacial cycle in a new pollen record from Lake Fimon (southern Alpine foreland, N-Italy). Quat. Sci. Rev. 29, 3115–3137.
Popescu, R., Urdea, P., Vespremeanu-Stroe, A., 2017. Deglaciation history of high Massifs from the Romanian Carpathians: towards an integrated view. In: Rădoane, M., Vespremeanu-Stroe, A. (Eds.), Landform Dynamics and Evolution in Romania. Springer Geography, pp. 87–116.
Pross, J., Koutsodendris, A., Christanis, K., Fischer, T., Fletcher, W.J., Hardiman, M., Kalaitzidis, S., Knipping, M., Kotthoff, U., Milner, A.M., Müller, U.C., Schmiedl, G., Siavalas, G., Tzedakis, P.C., Wulf, S., 2015. The 1.35-Ma-long terrestrial climate archive of Tenaghi Philippon, northeastern Greece: evolution, exploration, and perspectives for future research. Newsl. Stratigr. 48 (3), 253–276.
Pye, K., 1995. The nature, origin and accumulation of loess. Quat. Sci. Rev. 14, 653–667.
Pyle, D.M., Ricketts, G.D., Margari, V., van Andel, T.H., Sinitsyn, A.A., Praslov, N.D., Lisitsyn, S., 2006. Wide dispersal and deposition of distal tephra during the Pleistocene 'Campanian Ignimbrite/Y5' eruption, Italy. Quat. Sci. Rev. 25, 2713–2728.
Rasmussen, S.O., Andersen, K.K., Svensson, A.M., Steffensen, J.P., Vinther, B.M., Clausen, H.B., Siggaard-Andersen, M.-L., Johnsen, S.J., Larsen, L.B., Dahl-Jensen, D., Bigler, M., Röthlisberger, R., Fischer, H., Goto-Azuma, K., Hansson, M.E., Ruth, U., 2006. A new Greenland ice core chronology for the last glacial termination. J. Geophys. Res.: Atmosphere 111 (D6).
Rasmussen, S.O., Bigler, M., Blockley, S.P., Blunier, T., Buchardt, S.L., Clausen, H.B., Cvijanovic, I., Dahl-Jensen, D., Johnsen, S.J., Fischer, H., 2014. A stratigraphic framework for abrupt climatic changes during the Last Glacial period based on three synchronized Greenland ice-core records: refining and extending the INTIMATE event stratigraphy. Quat. Sci. Rev. 106, 14–28.
Ravazzi, C., Peresani, M., Pini, R., Vescovi, E., 2007. Il Tardoglaciale nelle Alpi italiane e in Pianura Padana. Evoluzione stratigrafica, storia della vegetazione e del popolamento antropico. Il Quat. 20 (2), 163–184.
Ravazzi, C., Badino, F., Marsetti, D., Patera, G., Reimer, P., 2012. Glacial to paraglacial history and forest recovery in the Oglio glacier system (Italian Alps) between 26 and 15 ka cal BP. Quat. Sci. Rev. 58, 146–161.
Reber, R., Akçar, N., Ivy-Ochs, S., Tikhomirov, D., Burkhalter, R., Zahno, C., Lüthold, A., Kubik, P.W., Vockenhuber, C., Schlüchter, C., 2014. Timing of retreat of the Reuss glacier (Switzerland) at the end of the last glacial maximum. Swiss J. Geosci. 107, 293–307.
Reille, M., de Beaulieu, J.L., 1990. Pollen analysis of a long upper Pleistocene continental sequence in a Velay maar (Massif Central, France). Palaeogeogr. Palaeoclimatol. Palaeoecol. 80 (1), 35–48.
Riel-Salvatore, J., Negrino, F., 2018. Human adaptations to climatic change in Liguria across the middle–upper Paleolithic transition. J. Quat. Sci. 33 (3), 313–322.
Rey-Rodríguez, I., López-García, J.M., Bennasar, M., Bañuls-Cardona, S., Blain, H.A., Blanco-Lapaz, Á., Rodríguez-Álvarez, X.-P., de Lombera-Hermida, A., Díaz-Rodríguez, M., Ameijenda-Iglesias, A., Agustí, J., Fábregas-Valcarce, R., 2016. Last Neanderthals and first anatomically modern humans in the NW Iberian peninsula: climatic and environmental conditions inferred from the Cova Eirós small-vertebrate assemblage during MIS 3. Quat. Sci. Rev. 151, 185–197.
Roche, D., Paillard, D., Cortijo, E., 2004. Constraints on the duration and freshwater release of Heinrich event 4 through isotope modelling. Nature 432 (7015), 379.
Ronchitelli, A., Boscato, P., Gambassini, P., 2009. Gli ultimi Neandertaliani in Italia: aspetti culturali. In: Facchini, F., Belcastro, G. (Eds.), La lunga storia di Neandertal. Biologia e comportamento. Jaka Book, Bologna, Italy, pp. 257–288.
Rossato, S., Monegato, G., Mozzi, P., Cucato, M., Gaudioso, B., Miola, A., 2013. Late Quaternary glaciations and connections to the piedmont plain in the prealpine environment: the middle and lower Astico Valley (NE Italy). Quat. Int. 288, 8–24.
Rossato, S., Carraro, A., Monegato, G., Mozzi, P., Tateo, F., 2018. Glacial dynamics in pre-Alpine narrow valleys during the Last Glacial Maximum inferred by lowland fluvial records (northeast Italy). Earth Surf. Dyn. 6, 809–828.
Roucoux, K.H., De Abreu, L., Shackleton, N.J., Tzedakis, P.C., 2005. The response of NW Iberian vegetation to North Atlantic climate oscillations during the last 65 kyr. Quat. Sci. Rev. 24 (14–15), 1637–1653.
Rousseau, D.-D., Derbyshire, E., Antoine, P., Hatté, C., 2018. European loess records. Ref. Modul. Earth Syst. Environ. Sci. 1–17.
Ruddiman, W.F., 1977. Late Quaternary deposition of ice-rafted sand in the subpolar North Atlantic (lat 40 to 65 N). Geol. Soc. Am. Bull. 88 (12), 1813–1827.
Ruszkiczay-Rüdiger, Z., Kern, Z., Urdea, P., Braucher, R., Madarász, B., Schimmelpfennig, I., 2016. Revised deglaciation history of the Pietrele-Stânişoara glacial complex, Retezat Mts, southern Carpathians, Romania. Quat. Int. 415, 216–229.
Ruth, U., Bigler, M., Röthlisberger, R., Siggaard-Andersen, M.L., Kipfstuhl, S., Goto-Azuma, K., Hansson, M.E., Johnsen, S.J., Lu, H., Steffensen, J.P., 2007. Ice core evidence for a very tight link between North Atlantic and east Asian glacial climate. Geophys. Res. Lett. 34 (3).
Sadori, L., Koutsodendris, A., Panagiotopoulos, K., Masi, A., Bertini, A., Combourieu-Nebout, N., Francke, A., Kouli, K., Joannin, S., Mercuri, A.M., Peyron, O., Torri, P., Wagner, B., Zanchetta, G., Sinopoli, G., Donders, T.H., 2016. Pollen-based paleoenvironmental and paleoclimatic change at Lake Ohrid (south-eastern Europe) during the past 500 ka. Biogeosciences 13, 1423–1437.
Salcher, B.C., Starnberger, R., Götz, J., 2015. The last and penultimate glaciation in the North Alpine Foreland: new stratigraphical and chronological data from the Salzach glacier. Quat. Int. 388, 218–231.
Sánchez Goñi, M.F., Eynaud, F., Turon, J.L., Shackleton, N.J., 1999. High resolution palynological record off the Iberian margin: direct land-sea correlation for the Last Interglacial complex. Earth Planet. Sci. Lett. 171 (1), 123–137.
Sánchez Goñi, M.F., Turon, J.L., Eynaud, F., Gendreau, S., 2000. European climatic response to millennial-scale changes in the atmosphere–ocean system during the Last Glacial period. Quat. Res. 54 (3), 394–403.
Sánchez Goñi, M.F., Cacho, I., Turon, J., Guiot, J., Sierro, F., Peypouquet, J., Grimalt, J., Shackleton, N., 2002. Synchroneity between marine and terrestrial responses to millennial scale climatic variability during the last glacial period in the Mediterranean region. Clim. Dyn. 19 (1), 95–105.
Sánchez Goñi, M.F., Landais, A., Fletcher, W.J., Naughton, F., Desprat, S., Duprat, J., 2008. Contrasting impacts of Dansgaard–Oeschger events over a western European latitudinal transect modulated by orbital parameters. Quat. Sci. Rev. 27 (11), 1136–1151.
Sánchez Goñi, M.F., Landais, A., Cacho, I., Duprat, J., Rossignol, L., 2009. Contrasting intrainterstadial climatic evolution between high and middle North Atlantic latitudes: a close-up of Greenland Interstadials 8 and 12. Geochem. Geophys. Geosyst. 10 (4).
Satow, C., Tomlinson, E.L., Grant, K.M., Albert, P.G., Smith, V.C., Manning, C.J., Ottolini, L., Wulf, S., Rohling, E.J., Lowe, J.J., Blockley, S.P.E., Menzies, M.A., 2015. A new contribution to the late quaternary tephrostratigraphy of the Mediterranean: Aegean sea core LC21. Quat. Sci. Rev. 117, 96–112.
Schneider, U., Becker, A., Finger, P., Meyer-Christoffer, A., Ziese, M., Rudolf, B., 2014. GPCC's new land surface precipitation climatology based on quality-controlled in situ data and its role in quantifying the global water cycle. Theor. Appl. Climatol. 115, 1–15.
Seguinot, J., Ivy-Ochs, S., Jouvet, G., Huss, M., Funk, M., Preusser, F., 2018. Modelling last glacial cycle ice dynamics in the Alps. Cryosphere 12, 3265–3285.
Seierstad, I.K., Abbott, P.M., Bigler, M., Blunier, T., Bourne, A.J., Brook, E., Buchardt, S.L., Buizert, C., Clausen, H.B., Cook, E., Dahl-Jensen, D., Davies, S.M., Guillevic, M., Johnsen, S.J., Pedersen, D.S., Popp, T.J., Rasmussen, S.O., Severinghaus, J.P., Svensson, A., Vinther, B.M., 2014. Consistently dated records from the Greenland GRIP, GISP2 and NGRIP ice cores for the past 104 ka reveal regional millennial-scale $\delta^{18}O$ gradients with possible Heinrich event imprint. Quat. Sci. Rev. 106, 29–46.

Seret, G., Dricot, E., Wansard, G., 1990. Evidence for an early glacial maximum in the French Vosges during the last glacial cycle. Nature 346, 453–456.
Serrano, E., Gómez-Lende, M., González-Amuchastegui, M.J., González-García, M., González-Trueba, J.J., Pellitero, R., Rico, I., 2015. Glacial chronology, environmental changes and implications for human occupation during the upper Pleistocene in the eastern Cantabrian Mountains. Quat. Int. 364, 22–34.
Sirocko, F., Knapp, H., Dreher, F., Förster, M.W., Albert, J., Brunck, H., Veres, D., Dietrich, S., Zech, M., Hambach, U., Röhner, M., Rudert, S., Schwibus, K., Adams, C., Sigl, P., 2016. The ELSA-Vegetation-Stack: reconstruction of Landscape Evolution Zones (LEZ) from laminated Eifel maar sediments of the last 60,000 years. Glob. Planet. Chang. 142, 108–135.
Smalley, I.J., Leach, J.A., 1978. The origin and distribution of the loess in the Danube basin and associated regions of East-Central Europe e a review. Sediment. Geol. 21, 1–26.
Spennato, A.G., 1981. I livelli protoaurignaziani della Grotta di Serra Cicora. Studi Ecol.l Quaternario 61, 52–76.
Spötl, C., Mangini, A., 2007. Speleothems and paleoglaciers. Earth Planet. Sci. Lett. 254 (3–4), 323–331.
Spötl, C., Mangini, A., Frank, N., Eichstädter, R., Burns, S.J., 2002. Start of the Last Interglacial period at 135 ka: evidence from a high alpine speleothem. Geology 30 (9), 815–818.
Staff, R.A., Hardiman, M., Ramsey, C.B., Adolphi, F., Hare, V.J., Koutsodendris, A., Pross, J., 2019. Reconciling the Greenland ice-core and radiocarbon timescales through the Laschamp geomagnetic excursion. Earth Planet. Sci. Lett. 520, 1–9.
Starkovich, B.M., 2017. Paleolithic subsistence strategies and changes in site use at Klissoura Cave 1 (Peloponnese, Greece). J. Hum. Evol. 111, 63–84.
Staubwasser, M., Drăgușin, V., Onac, B.P., Assonov, S., Ersek, V., Hoffmann, D.L., Veres, D., 2018. Impact of climate change on the transition of Neanderthals to modern humans in Europe. Proc. Natl. Acad. Sci. 115 (37), 9116–9121.
Steegmann Jr., A.T., Cerny, F.J., Holliday, T.W., 2002. Neandertal cold adaptation: physiological and energetic factors. Am. J. Hum. Biol. 14 (5), 566–583.
Steffensen, J.P., Andersen, K.K., Bigler, M., Clausen, H.B., Dahl-Jensen, D., Fischer, H., Goto-Azuma, K., Hansson, M., Johnsen, S.J., Jouzel, J., Masson-Delmotte, V., Popp, T., Rasmussen, S.O., Röthlisberger, R., Ruth, U., Stauffer, B., Siggaard-Andersen, M.-L., Sveinbjörnsdóttir, A.E., Svensson, A., White, J.W.C., 2008. High-resolution Greenland ice core data show abrupt climate change happens in few years. Science 321 (5889), 680–684.
Stern, J.V., Lisiecki, L.E., 2013. North Atlantic circulation and reservoir age changes over the past 41,000 years. Geophys. Res. Lett. 40 (14), 3693–3697.
Stiner, M.C., Kozowski, J.K., Kuhn, S.L., Karkanas, P., Koumouzelis, M., 2007. Klissoura cave 1 and the upper Paleolithic of southern Greece in cultural and ecological context. Eurasian Prehistory 7, 309–321.
Stoll, H.M., Moreno, A., Mendez-Vicente, A., Gonzalez-Lemos, S., Jimenez-Gochez, M., Dominguez-Cuesta, M.J., Edwards, R.L., Cheng, H., Wang, X., 2013. Paleoclimate and growth rates of speleothems in the northwestern Iberian Peninsula over the last two glacial cycles. Quat. Res. 80 (2), 284–290.
Svensson, A., Andersen, K.K., Bigler, M., Clausen, H.B., Dahl-Jensen, D., Davies, S.M., Johnsen, S.J., Muscheler, R., Parrenin, F., Rasmussen, S.O., Röthlisberger, R., Seierstad, I., Steffensen, J.P., Vinther, B.M., 2008. A 60,000 year Greenland stratigraphic ice core chronology. Clim. Past 4, 47–57.
Temovski, M., Madarász, B., Kern, Z., Milevski, I., Ruszkiczay-Rüdiger, Z., 2018. Glacial geomorphology and Preliminary glacier reconstruction in the Jablanica mountain, Macedonia, central Balkan peninsula. Geosciences 8, 270. https://doi.org/10.3390/geosciences8070270.
Terhorst, B., Sedov, S., Sprafke, T., Peticzka, R., Meyer-Heintze, S., Kühn, P., Solleiro Rebolledo, E., 2015. Austrian MIS 3/2 loess–palaeosol records-Key sites along a west–east transect. Palaeogeogr. Palaeoclimatol. Palaeoecol. 418, 43–56.
Thiel, C., Horváth, E., Frechen, M., 2014. Revisiting the loess/palaeosol sequence in Paks, Hungary: a post-IR IRSL based chronology for the 'Young Loess Series'. Quat. Int. 319, 88–98.
Timar, A., Vandenberghe, D., Panaiotu, E.C., Panaiotu, C.G., Necula, C., Cosma, C., van den Haute, P., 2010. Optical dating of Romanian loess using fine-grained quartz. Quat. Geochronol. 5 (2–3), 143–148.
Timar-Gabor, A., Vandenberghe, D.A.G., Vasiliniuc, S., Panaoitu, C.E., Panaiotu, C.G., Dimofte, D., Cosma, C., 2011. Optical dating of Romanian loess: a comparison between silt-sized and sand-sized quartz. Quat. Int. 240, 62–70.
Tinner, W., Hubschmid, P., Wehrli, M., Ammann, B., Conedera, M., 1999. Long-term forest fire ecology and dynamics in southern Switzerland. J. Ecol. 87, 273–289.
Toucanne, S., Soulet, G., Freslon, N., Jacinto, R.S., Dennielou, B., Zaragosi, S., Eynaud, F., Bourillet, J.-F., Bayon, Germain, 2015. Millennial-scale fluctuations of the European Ice Sheet at the end of the last glacial, and their potential impact on global climate. Quat. Sci. Rev. 123, 113–133.
Tranquillini, W., 1979. General features of the upper timberline. In: Physiological Ecology of the Alpine Timberline Springer Berlin Heidelberg, pp. 1–4.
Turkish State Meteorological Service, 2006. Climate of Turkey. Turkish State Meteorological Service. Archived from the Original on April 19, 2008. Retrieved 2006-12-27.
Tzedakis, P.C., 1999. The last climatic cycle at Kopais, central Greece. J. Geol. Soc. 156 (2), 425–434.
Tzedakis, P.C., Lawson, I.T., Frogley, M.R., Hewitt, G.M., Preece, R.C., 2002. Buffered tree population changes in a Quaternary refugium: evolutionary implications. Science 297 (5589), 2044–2047.
Tzedakis, P.C., Frogley, M.R., Lawson, I.T., Preece, R.C., Cacho, I., De Abreu, L., 2004. Ecological thresholds and patterns of millennial-scale climate variability: the response of vegetation in Greece during the last glacial period. Geology 32 (2), 109–112.
Tzedakis, P.C., Hooghiemstra, H., Pälike, H., 2006. The last 1.35 million years at Tenaghi Philippon: revised chronostratigraphy and long-term vegetation trends. Quat. Sci. Rev. 25 (23–24), 3416–3430.
Valen, V., Larsen, E., Mangerud, J.A.N., 1995. High-resolution paleomagnetic correlation of Middle Weichselian ice-dammed lake sediments in two coastal caves, western Norway. Boreas 24 (2), 141–153.
van Andel, T.H., Tzedakis, P.C., 1998. Priority and opportunity: reconstructing the European Middle Palaeolithic climate and landscape. In: Bailey, J. (Ed.), Science in Archaeology. An Agenda for the Future, pp. 37–45 English Heritage.
van Andel, T.H., Davies, W., Weninger, B., 2003. The human presence in Europe during the last glacial period I: human migrations and the changing climate. Neanderthals and modern humans in the European landscape during the last glaciation: archaeological results of the Stage 3, 31–56.
Van Meerbeeck, C.J., Renssen, H., Roche, D.M., Wohlfarth, B., Bohncke, S.J.P., Bos, J.A.A., Engels, S., Helmens, K.F., Sánchez Goñi, F., Svensson, A., Vandenberghe, J., 2011. The nature of MIS 3 stadial-interstadial transitions in Europe: new insights from model-data comparison. Quat. Sci. Rev. 30, 3618–3637.
Verheul, J., Zickel, M., Becker, D., Willmes, C., 2015. LGM Major Inland Waters of Europe-GIS Dataset. CRC806-Database. pp. 14. https://doi.org/10.5880/SFB806.
Villa, P., Roebroeks, W., 2014. Neandertal demise: an archaeological analysis of the modern human superiority complex. PLoS One 9 (4), e96424.
Wacha, L., Pavlaković, S.M., Frechen, M., Crnjaković, M., 2011a. The loess chronology of the island of Susak, Croatia. E&G Quaternary Science Journal 60, 153–169.
Wacha, L., Pavlakovic, S., Novothny, A., Crnjaković, M., Frechen, M., 2011b. Luminescence dating of upper Pleistocene loess from the island of Susak in Croatia. Quat. Int. 234, 50–61.
Waelbroeck, C., Labeyrie, L., Michel, E., Duplessy, J.C., Lambeck, K., McManus, J.F., Balbon, E., Labracherie, M., 2002. Sea-level and deep water temperature changes derived from benthic foraminifera isotopic records. Quat. Sci. Rev. 21, 295–305.
Wainer, K., Genty, D., Blamart, D., Hoffmann, D., Couchoud, I., 2009. A new stage 3 millennial climatic variability record from a SW France speleothem. Palaeogeogr. Palaeoclimatol. Palaeoecol. 271 (1), 130–139.
Walter, H., Breckle, S.W., 1986. Spezielle Ökologie der gemässigten und arktischen Zonen Euro-Nordasiens: Zonobiom VI-IX. (Fischer).
Weber, M., Scholz, D., Schröder-Ritzrau, A., Deininger, M., Spötl, C., Lugli, F., Mertz-Kraus, R., Jochum, K.P., Fohlmeister, J., Stumpf, C.F., Riechelmann, D.F.C., 2018. Evidence of warm and humid interstadials in central Europe during early MIS 3 revealed by a multi-proxy speleothem record. Quat. Sci. Rev. 200, 276–286.
Whitlock, C., Larsen, C., 2001. Charcoal as a fire proxy. In: Smol, J.P., Birks, H.J.B., Last, W.M. (Eds.), Tracking Environmental Change Using Lake Sediments. vol. 3. pp. 75–97 Terrestrial, algal, and Siliceous Indicators.
Wijmstra, T.A., 1969. Palynology of the first 30 metres of a 120 m deep section in northern Greece. Acta Bot. Neerl. 18 (4), 511–527.
Wohlfarth, B., 2010. Ice-free conditions in Sweden during marine oxygen isotope stage 3? Boreas 39 (2), 377–398.
Woillard, G.M., 1978. Grande Pile peat bog: a continuous pollen record for the last 140,000 years. Quat. Res. 9, 1–21.
Wood, R., 2015. From revolution to convention: the past, present and future of radiocarbon dating. J. Archaeol. Sci. 56, 61–72.
Wood, R.E., Douka, K., Boscato, P., Haesaerts, P., Sinitsyn, A., Higham, T., 2012. Testing the ABOx-SC method: dating known-age charcoals associated with the Campanian Ignimbrite. Quat. Geochronol. 9, 16–26.
Wroe, S., Parr, W.C., Ledogar, J.A., Bourke, J., Evans, S.P., Fiorenza, L., Benazzi, S., Hublin, J.-J., Stringer, C., Kullmer, O., Curry, M., Rae, T.C., Yokley, T.R., 2018. Computer simulations show that Neanderthal facial morphology represents adaptation to cold and high energy demands, but not heavy biting. Proceedings Royal Society B 285 (1876), 20180085.
Wulf, S., Hardiman, M.J., Staff, R.A., Koutsodendris, A., Appelt, O., Blockley, S.P., Lowe, J.J., Manning, C.J., Ottolini, L., Schmitt, A.K., Smith, V.C., Tomlinson, E.L., Vakhrameeva, P., Knipping, M., Kotthoff, U., Milner, A.M., Müller, U.C., Christanis, K., Kalaitzidis, S., Tzedakis, P.C., Schmiedl, G., Pross, J., 2018. The marine isotope stage 1–5 cryptotephra record of Tenaghi Philippon, Greece: towards a detailed tephrostratigraphic framework for the Eastern Mediterranean region. Quat. Sci. Rev. 186, 236–262.
Wutke, K., Wulf, S., Tomlinson, E.L., Hardiman, M., Dulski, P., Luterbacher, J., Brauer, A., 2015. Geochemical properties and environmental impacts of seven Campanian tephra layers deposited between 40 and 38 ka BP in the varved lake sediments of Lago Grande di Monticchio, southern Italy. Quat. Sci. Rev. 118, 67–83.
Yazbeck, C., 2004. Le Paleolithique du Liban: bilan critique. Paleorient 30, 111–126.
Zanchetta, G., Giaccio, B., Bini, M., Sarti, L., 2018. Tephrostratigraphy of Grotta del Cavallo, Southern Italy: insights on the chronology of Middle to Upper Palaeolithic transition in the Mediterranean. Quat. Sci. Rev. 182, 65–77.
Zasadni, J., Klapyta, P., 2014. The Tatra mountains during the last glacial maximum. J. Maps 10 (3), 440–456.
Žebre, M., Stepišnik, U., 2014. Reconstruction of late Pleistocene glaciers on mount Lovćen, Montenegro. Quat. Int. 353, 225–235.
Žebre, M., Stepišnik, U., 2015. Glaciokarst geomorphology of the northern Dinaric alps: Snežnik (Slovenia) and Gorski Kotar (Croatia). J. Maps 5, 873–881. https://doi.org/10.1080/17445647.2015.1095133.
Žebre, M., Stepišnik, U., Colucci, R.R., Forte, E., Monegato, G., 2016. Evolution of a karst polje influenced by glaciation: the Gomance piedmont polje (northern Dinaric Alps). Geomorphology 257, 143–154.
Žebre, M., Jež, J., Mechernich, S., Mušič, B., Horn, B., Jamšek Rupnik, P., 2019. Paraglacial adjustment of alluvial fans to the last deglaciation in the Snežnik Mountain, Dinaric karst (Slovenia). Geomorph 332, 66–79.
Zerboni, A., Trombino, L., Frigerio, C., Livio, F., Berlusconi, A., Michetti, A.M., Rodnight,

H., Spötl, C., 2015. The loess -paleosol sequence at Monte Netto: a record of climate change in the Upper Pleistocene of the central Po Plain, northern Italy. J. Soils Sediments 15, 1329–1350.
Zerboni, A., Amit, R., Baroni, C., Coltorti, M., Ferrario, M.F., Fioraso, G., Forno, M.G., Frigerio, C., Gianotti, F., Irace, A., Livio, F., Mariani, G.S., Michetti, A.M., Monegato, G., Mozzi, P., Orombelli, G., Perego, A., Porat, N., Rellini, I., Trombino, L., Cremaschi, M., 2018. Towards a map of the upper Pleistocene loess of the Po plain loess basin (northern Italy). Alpine and Mediterranean Quaternary 31, 253–256.
Zhornyak, L.V., Zanchetta, G., Drysdale, R.N., Hellstrom, J.C., Isola, I., Regattieri, E., Piccini, L., Baneschi, I., Couchoud, I., 2011. Stratigraphic evidence for a “pluvial phase” between ca 8200–7100 ka from Renella cave (Central Italy). Quat. Sci. Rev. 30 (3–4), 409–417.
Zilhão, J., Bank, s W.E., d'Errico, F., Gioia, P., 2015. Analysis of site formation and assemblage integrity does not support attribution of the Uluzzian to modern humans at Grotta del Cavallo. PLoS One 10 (7), e0131181.